

**EXPERIMENTAL STUDIES ON SOLID-LIQUID MASS TRANSFER  
IN  
PACHUCA TANKS**

*A Thesis Submitted  
in Partial Fulfilment of the Requirements  
for the Degree of*  
**MASTER OF TECHNOLOGY**

*by*  
**CHANDRASEKHAR T**

*to the*  
**DEPARTMENT OF MATERIALS AND METALLURGICAL ENGINEERING  
INDIAN INSTITUTE OF TECHNOLOGY KANPUR**  
*June, 1994*

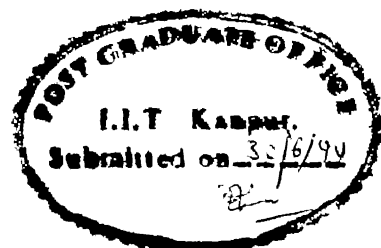
5 1 SEP 1994  
CENTRAL LIBRARY  
IIT KANPUR  
Call No. A. 118182

MME-1994-M-CHA-EXP



A118182

CERTIFICATE



This is to certify that the present work, entitled "Experimental Studies on Solid-liquid Mass Transfer in Pachuca Tanks" by Torlikonda Chandrasekhar has been carried out under our supervision and it has not been submitted elsewhere for a degree.

*Raj Shekhar*

Dr. Rajiv Shekhar

Asst. Professor

Department of Materials and Metallurgical Engineering

Indian Institute of Technology

Kanpur - 208016

*S.P. Mehrotra*

Dr. S.P. Mehrotra

Professor

June, 1994

I take this opportunity to express my deep sense of indebtedness and gratitude to Dr. S.P.Mehrotra and Dr. Rajiv Shekhar who had given me invaluable guidance and helped me in every possible way to complete this work.

I am thankful to my senior Mr. G.G.Roy for the useful discussions I had with him related to my work and to Mr. G.P.Bajpai and Mr. A.K.Gupta for their constant help while carrying out the experiments. I express my special thanks to Mr. D.N.Patel and Mr. K.S.Rao for their help in submitting the thesis.

Thanks are also due to my friends Govind, Umasankar, Sitharam, Gummadi and Banu whose memories I would like to cherish throughout my life. I express my sincere thanks to Mr. A.Sharma, D.P.Tripathi and K.S.Tripathi for being available in times of need.

More than anybody else, I am greatful to my parents and sisters for their inspiration and encouragement throughout my study, and it is to them that this work is dedicated.

## TABLE OF CONTENTS

ABSTRACT	i
LIST OF FIGURES	iii
LIST OF TABLES	vi
NOMENCLATURE	vii
CHAPTER 1. INTRODUCTION	
1.1. Previous Investigations	7
1.1.1 Mechanically agitated tanks	8
1.1.2 Air aigitated tanks	13
1.2. Research Objective	18
CHAPTER 2. EXPERIMENTAL APPARATUS AND MEASUREMENTS	19
2.1. Experimental Apparatus and Calibration	21
2.1.1 Mechanically agitated tanks	21
2.1.2 Pachuca tank	24
2.2. Conductivity measurements	26
2.2.1 Calibration of conductivity cell	26
2.2.2 Response rate of conductivity cell	29
2.3. Experimental measurements	29
2.3.1 Measurement of mass transfer coefficient - theory	29
2.3.2 Correlation between molfraction( $Y_b$ ) and solution conductivity	32
2.4. Experimental conditions	34
2.5. Experimental procedure	39
2.5.1 Superficial Gas Velocity	39
2.5.2 Position of conductivity probe	39
2.5.3 Position of air inlet & draft tube	40
2.5.4 Effect of submergence of the draft tube	41
2.5.5 Configuration for Free Air-lift tanks	42

CHAPTER 3. RESULTS AND DISCUSSION	44
3.1. Mechanical agitation	44
3.1.1 Effect of Stirrer speed on $K_{st}$	44
3.1.2 Effect of baffles on $K_{st}$	46
3.1.3 Effect of particle size on $K_{st}$	51
3.1.4 Correlation between power input and $K_{st}$	51
3.2. Air agitation	55
3.2.1 Effect of superficial gas velocity on $K_{st}$	55
3.2.2 Effect of height to diameter ratio on $K_{st}$	62
3.2.3 Effect of draft tube diameter on $K_{st}$	68
3.2.4 Correlation between power input and $K_{st}$	71
3.2.5 Stub column tanks	76
3.2.5 Free air-lift tanks	79
3.2.6 Comparison of FCC,FAL and SC configurations	82
3.2.7 Comparison of air and mechanically agitated tanks interms of power input	82
CHAPTER 4. CONCLUSIONS	87

APPENDIX

REFERENCES

## ABSTRACT

Solid/liquid mass transfer of reactant species from bulk liquid to the solid/liquid interface or vice versa, may be an important kinetic step in leaching. The objective of the present investigation has been to characterize solid-liquid mass transfer coefficient ( $K_{sl}$ ) as a function of design and operating parameters in pachuca tanks such as superficial gas velocity ( $U_g$ ), height to diameter ratio of liquid column ( $H_t/D_t$ ) and a ratio of draft tube to tank diameter ( $D_d/D_t$ ). In addition the effect of tank design on the mass transfer coefficient has been studied using a tank with a foreshortened draft tube and a tank without the draft tube, as both these are also important from industrial point of view.

Initially, a series of experiments have been carried out in a mechanically agitated tanks to select the conditions that would promote external mass transport. In addition, the effect of different operating parameters such as stirrer speed, temperature, particle size and effect of baffles on the mass transfer coefficient has been studied. This has been done mainly to compare the performance of air agitated and mechanically agitated tanks in terms of energy input per unit volume to the system.

Irrespective of the design of the tank i.e. Full centred column (FCC), stub column (SC) and free air-lift (FAL) pachucas, the mass transfer coefficient was observed to increase with  $U_g$ . In FCC tanks  $K_{sl}$  has shown an optimum with respect to  $H_t/D_t$ , giving the maximum at a value of  $H_t/D_t$  equal to 2.0. Whereas in FAL and SC pachucas monotonical increase was observed with increase in  $H_t/D_t$ . Furthermore,  $K_{sl}$  also increased with the draft tube diameter, keeping the tank diameter constant. At lower  $H_t/D_t$  ratios,  $K_{sl}$  was observed to be independent of configuration in FCC and SC tanks, while at higher values of this ratio SC tanks were noted to be more effective

than FCC tanks in terms of mass transfer. Finally air agitated tanks were observed to be superior in terms of power input per unit volume of the system, to that of mechanically agitated tanks.

## LIST OF FIGURES

<u>FIGURE NO</u>	<u>TITLE</u>	<u>PAGE NO</u>
1.1	Flow pattern in mechanically agitated tanks	3
1.2	Classification of Pachuca tanks	6
2.1	Experimental set-up - Mechanically agitated tank	22
2.2	Calibration of Mechanical stirrer	23
2.3	Experimental set-up - Air agitated tank (Pachuca)	25
2.4	Calibration of Capillary flowmeters	27
2.5	Calibration of conductivity cell	28
2.6	Typical chart recorder traces with different concentrations of aqueous solution	30
2.7	Typical chart recorder traces with different percentages of resin	30
2.8	A plot between pH and conductance	33
2.9	Correlation between molfraction of $K^+$ and conductance	33
2.10	Effect of the concentration of aqueous solution on $K_{sl}$ at 1200rpm	36
2.11	Effect of the concentration of aqueous solution on $K_{sl}$ at 1500rpm	36
2.12	Typical activation energy curve for ion exchange reaction	38
2.13	Effect of temperature on $K_{sl}$	38
2.14	Experimental set-up for Free Air-lift tanks	43
3.1	Effect of stirrer speed on $K_{sl}$	47
3.2	Experimental set up for Baffled tank	49
3.3	Effect of Baffles on $K_{sl}$	50
3.4	Effect of Particle size on $K_{sl}$	52
3.5	Comparison between measured and predicted values of $K_{sl}$ (unbaffled condition)	54

<u>FIGURE NO</u>	<u>TITLE</u>	<u>PAGE NO</u>
3.6	Comparison between measured and predicted values of $K_{sl}$ (baffled condition)	54
3.7	Effect of superficial gas velocity on $K_{sl}$ with $D_d/D_t = 0.08$ in FCC tanks	56
3.8	Effect of superficial gas velocity on $K_{sl}$ with $D_d/D_t = 0.18$ in FCC tanks	56
3.9	Effect of superficial gas velocity on $K_{sl}$ with $D_d/D_t = 0.30$ in FCC tanks	57
3.10	Effect of superficial gas velocity on $U_{la}$ with $D_d/D_t = 0.08$ in FCC tanks	60
3.11	Effect of superficial gas velocity on $U_{la}$ with $D_d/D_t = 0.18$ in FCC tanks	60
3.12	Effect of superficial gas velocity on $U_{la}$ with $D_d/D_t = 0.30$ in FCC tanks	61
3.13	Effect of the liquid column height on $K_{sl}$ with $D_d/D_t = 0.08$ in FCC tanks	63
3.14	Effect of the liquid column height on $K_{sl}$ with $D_d/D_t = 0.18$ in FCC tanks	63
3.15	Effect of the liquid column height on $K_{sl}$ with $D_d/D_t = 0.30$ in FCC tanks	64
3.16	Effect of height of the liquid column on $U_{la}$ with $D_d/D_t = 0.08$ in FCC tanks	66
3.17	Effect of height of the liquid column on $U_{la}$ with $D_d/D_t = 0.18$ in FCC tanks	66
3.18	Effect of height of the liquid column on $U_{la}$ with $D_d/D_t = 0.30$ in FCC tanks	67
3.19	Effect of the draft tube diameter on $K_{sl}$ with $H_t/D_t = 1.5$ in FCC tanks	69

<u>FIGURE NO</u>	<u>TITLE</u>	<u>PAGE NO</u>
3.20	Effect of the draft tube diameter on $K_{sl}$ with $H_t/D_t = 2.0$ in FCC tanks	69
3.21	Effect of the draft tube diameter on $K_{sl}$ with $H_t/D_t = 2.5$ in FCC tanks	70
3.22	Effect of the draft tube diameter on $U_{la}$ with $H_t/D_t = 1.5$ in FCC tanks	72
3.23	Effect of the draft tube diameter on $U_{la}$ with $H_t/D_t = 2.0$ in FCC tanks	72
3.24	Effect of the draft tube diameter on $U_{la}$ with $H_t/D_t = 2.5$ in FCC tanks	73
3.25	Comparison between measured and predicted values of $K_{sl}$ (Single variable correlation)	75
3.26	Comparison between measured and predicted values of $K_{sl}$ (Multi-variable correlation)	75
3.27	Effect of superficial gas velocity on $K_{sl}$ in SCT tanks	78
3.28	Effect of tank height on $K_{sl}$ in SCT tanks	78
3.29	Effect of Superficial gas velocity on $K_{sl}$ in FAL tanks	80
3.30	Effect of tank Height on $K_{sl}$ in FAL tanks	80
3.31	Effect of tank design on $K_{sl}$ at $H_t/D_t = 1.5$	83
3.32	Effect of tank design on $K_{sl}$ at $H_t/D_t = 2.0$	83
3.33	Effect of tank design on $K_{sl}$ at $H_t/D_t = 2.5$	84
3.34	Comparison of air and mechanically agitated tanks	86

## LIST OF TABLES

<u>TABLE NO</u>	<u>TITLE</u>	<u>PAGE NO</u>
1	Industrial survey of pachuca tanks by Hallett and coworkers	17
2	Design and operating parameters used in Industrial and Laboratory Pachuca tanks	20
3	Ranges of design and operating parameters in present study	45

## NOMENCLATURE

FCC	full centred-column
SCT	stub column type
FAL	free air-lift
A	surface area, $\text{m}^2$
$A_d$	area of cross section of the draft tube, $\text{m}^2$
$A_a$	area of cross section of the annulus, $\text{m}^2$
$C_p$	initial concentration of solution, $\text{mol}/\text{m}^3$
D	diffusion coefficient in solution, $\text{m}^2/\text{sec}$
$\bar{D}$	diffusion coefficient in ion exchanger, $\text{m}^2/\text{sec}$
$D_d$	diameter of the draft tube, $\text{m}$
$D_t$	diameter of the tank, $\text{m}$
$d_p$	diameter of the resin particle, $\text{m}$
$f_d$	frictional factor, --
g	acceleration due to gravity, $\text{m}/\text{sec}^2$
$H_d$	height of the draft tube, $\text{m}$
$H_l$	height of the liquid column, $\text{m}$
$K_{sl}$	solid-liquid mass transfer coefficient, $\text{m}/\text{sec}$
$K_{gl}$	gas-liquid mass transfer coefficient, $\text{m}/\text{sec}$
$k_{ru}$	coefficient of frictional loss at the top of draft tube
$k_{rl}$	coefficient of frictional loss at bottom of draft tube
N	speed of stirrer, rpm
$P_{atm}$	pressure, $\text{Kg}/\text{m}^2$
P	power number, --
Q	gas flow rate, $\text{m}^3/\text{sec}$
t	time, sec
T	stirrer diameter, $\text{m}$
T	temperature, $^{\circ}\text{C}$

$T_t$	temperature of the solution, $^{\circ}\text{C}$
$U_{la}$	superficial liquid velocity in the annulus, m/sec
$U_{ld}$	superficial liquid velocity in draft tube, m/sec
$U_g$	superficial gas velocity, m/sec
$U$	absolute velocity, m/sec
$V$	volume of the liquid, $\text{m}^3$
$W$	weight of resin, gm
$X$	concentration of fixed ionic groups in resin, $\text{mol}/\text{m}^3$
$Y_b$	molfraction of $\text{K}^+$ ions in bulk solution, --
$Y_i$	molfraction of $\text{K}^+$ ions at solid-liquid interface, --
Re	Reynolds number
Sc	Scmidtz number
Sh	Sherwood number

#### Greek Symbols

$\phi_{a,d}$	gas hold-up in the annulus and draft tube
$\varepsilon$	power input per unit volume, $\text{Kg}/\text{m sec}^3$
$\mu$	molecular viscosity, $\text{Kg}/\text{m sec}$
$\nu$	kinematic viscosity, $\text{m}^2/\text{sec}$
$\rho$	density, $\text{Kg}/\text{m}^3$
$\sigma$	specific conductance, $\text{mmho}/\text{cm}$
$\delta$	boundary layer thickness, m
$\alpha$	separation factor, --

## CHAPTER I

### INTRODUCTION

In a solid/liquid reaction, the overall process will involve the following kinetic steps : (a) mass transfer of the reactants and products between the bulk of the fluid and external surface of the solid particle, (b) diffusion of the reactants and products within the pores of solid, and (c) chemical reaction between the reactants in the fluid and the solid. The slowest of these steps controls the overall rate of reaction and the system is called, respectively, external mass transfer controlled, intraparticle or pore diffusion controlled and reaction rate controlled. It has been recognized that the rate controlling step can change depending upon reaction conditions. Solid/liquid mass transfer, that is transport of species from bulk to the solid/liquid interface or vice-versa, may be an important kinetic step in leaching.

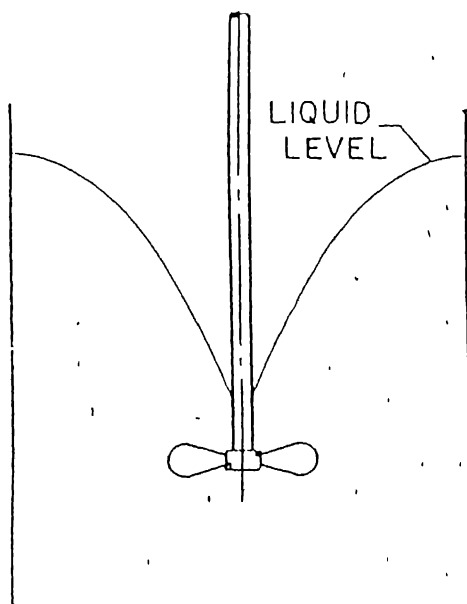
In Hydrometallurgical systems, involving dissolution or precipitation of solid, diffusion through a zone adjacent to the solid/liquid interface (boundary layer) may be rate controlling. Under constant conditions of agitation the thickness of the zone decreases and a steady state condition is soon attained in which

most the of material entering the zone balances that leaving the zone.

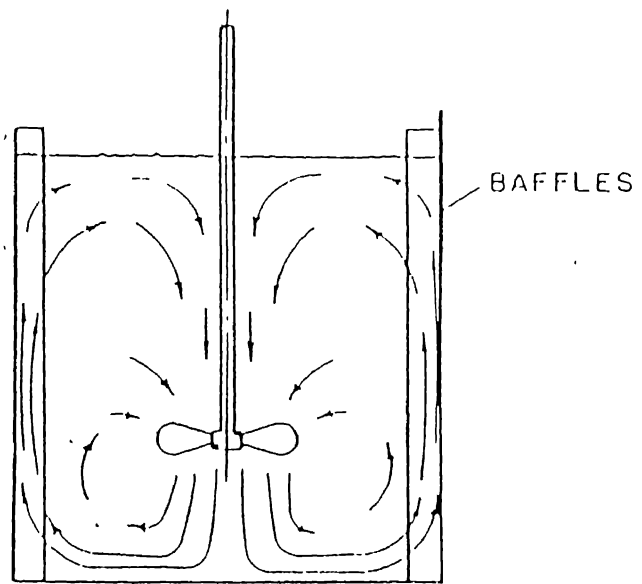
The main objectives of agitation in solid-liquid system can be classified as, uniform suspension of solid particles in liquid and reduction of diffusion resistance around solid particles. The uniform suspension of solid particles is not easily attained and also is not always required. Although there are some cases where homogeneous slurries are desired, once all the particles are suspended the latter may become important for dissolution of solids in liquid.

In general, agitation is created in industrial tanks by two methods: (1)Mechanical stirring and (2)Air agitation. Sometimes a combination of these two methods may be used. Hence, both the systems will be dealt with here.

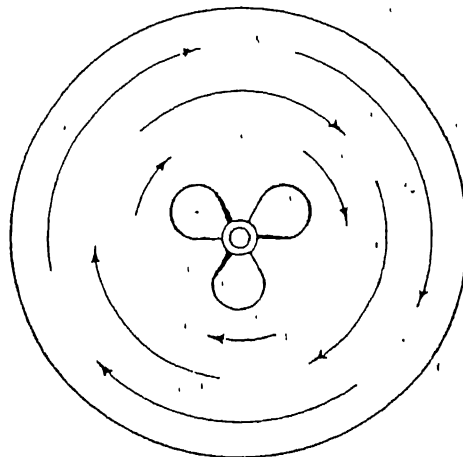
Mechanical Agitation : In mixing vessels to produce agitation (mixing) it is necessary to supply energy and this is usually accomplished through the rotation of an impeller. In these vessels the flow pattern and power consumed are not only dependent upon the type of impeller used and how rapidly it is rotated but also on physical properties of the fluid, shape of the container, relative position of baffles etc. Baffles are generally used to get higher mixing rates at the cost of energy input. Fig.1.1 shows the flow



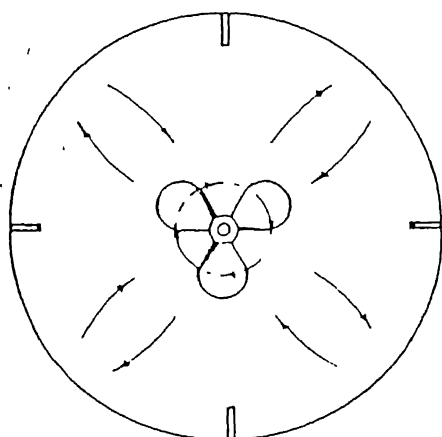
SIDE VIEW



SIDE VIEW



BOTTOM VIEW



BOTTOM VIEW

Fig.1.1 Flow pattern in mechanically agitated tanks

pattern in the vessels equipped with and without baffles. Depending on design, the impellers are classified as propellers, turbines and paddles. In our case a three-bladed propeller was used for mechanical agitation.

Air Agitation (Pachuca Tank) : The most commonly used air agitated vessels in hydrometallurgy are the Pachuca Tanks which are described in detail below: Pachuca tanks are used in Hydrometallurgical industries as leaching reactors for production of nonferrous metals such as uranium, gold, zinc and copper. The principal objectives in operation of these reactors are the suspension of particles, mixing of reagents, mass transfer between the solution and particle, and mass transfer between air bubbles and slurry. Air(gas) agitated reactors are also used in other process industries, particularly in chemical and biochemical fields, where they are known as bubble columns or air lift reactors. In the steel plants argon is used to stir molten metal in ladles for degasification and homogenization.

The main difference between Pachuca tank, bubble column and argon stirred ladle is in terms of size and geometry. Pachuca tanks are cylindrical in cross-section with a conical bottom, up to about 10m high and 10m in diameter. Argon stirred ladles seldom exceed 2-4m in diameter and bubble columns are even smaller. With

values ranging from 1.5 to 4, the  $H_t/D_t$  ratio of pachucas fall between those of argon stirred ladles and bubble columns.

Air lifts or draft tubes, which are typically 30cm in diameter with both ends open, run parallel to the length of the tank and situated just above the air inlet. Pachuca tanks are classified in terms of draft tubes as (see Fig.1.2),

(1)Full Center Column(FCC) : the draft tube extend from just above the air injection point in the cone to just below the liquid surface

(2)Stub Column type Tanks(SCT) : this consists of a foreshortened draft tube ending just above the cone

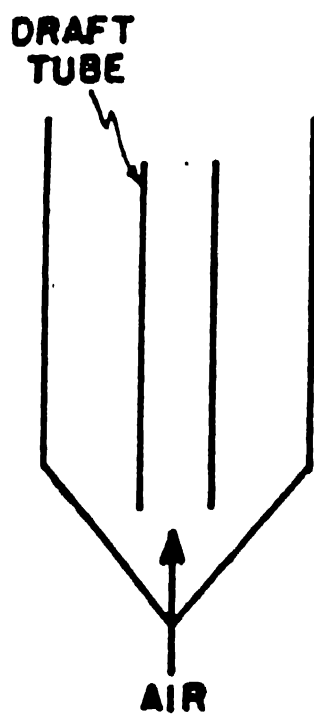
(3)Free Air-lifts(FAL) : here the draft tube is absent.

Air agitated tanks have got some inherent advantages over mechanically agitated systems namely,

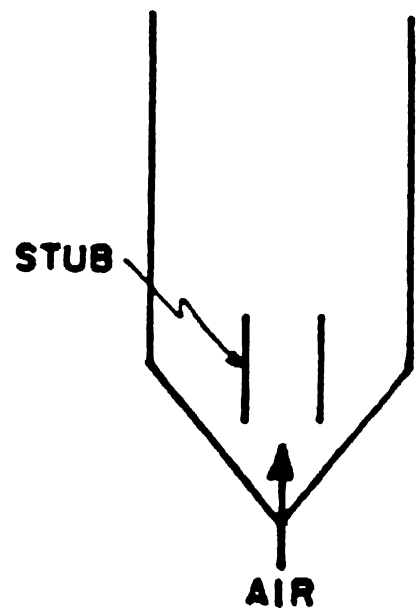
(a)they have no moving parts and can be used for the treatment of corrosive liquids and abrasive slurries without any danger of corrosion and erosion, and

(b)aeration of the pulp can be readily provided for enhanced dissolution rates as in the leaching of gold and the carbonate leaching of uranium.

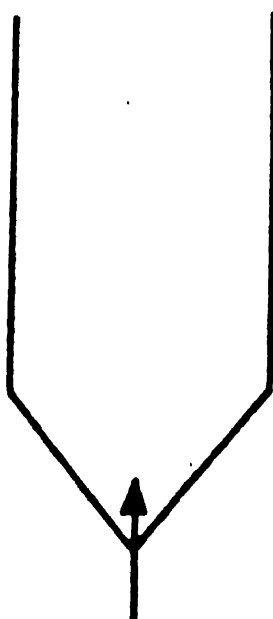
However, liquid agitation by air sparging is reported to be milder than mechanical agitation and is not applicable for



FULL CENTER COLUMN



STUB COLUMN



FREE AIRLIFT

Fig.1.2 Classification of Pachuca tanks

liquids having higher viscosity values.

Mass transfer depends on the liquid velocities and the turbulence levels in the tank, which vary with the design and operating parameters of tank. Therefore it is essential to study the effect of design and operating conditions of the reactor that will effect the mass transfer coefficient and consequently optimize the parameters for effective dissolution.

### 1.1 PREVIOUS INVESTIGATIONS

---

The aim of the study has been to study solid/liquid mass transfer in both air and mechanically agitated tanks and subsequently correlate the results in terms of power input to the system and design and operating parameters. Therefore it is essential to understand how  $K_{sl}$  varies with operational variables such as superficial gas velocity, height to diameter ratio of liquid column, etc. In addition, before conducting the experiments it is important to identify operational variables that affect the process parameters. Therefore, this chapter mainly deals with experimental measurements in the literature regarding solid-liquid mass transfer in mechanical and air agitated tanks. Finally, we look at the hydrodynamics in pachuca tanks with and without draft tube, which is essential for experimental measurements and predictions.

### 1.1.1 MECHANICALLY AGITATED TANKS

---

Extensive work has been done on rates of mass transfer from or to solid particles suspended in agitated liquids. Experimental conditions have been chosen so as to minimize the effect of any solid side mass transfer resistance. In principle this condition can be obtained by using dilute solutions and a small percentage of solids. The available literature shows that mass transfer coefficient can vary with the following parameters : stirrer speed or power input, particle size, diffusivity of the aqueous solution, density difference between liquid and solid, viscosity of liquid and also turbine size and design.

1.1.1.1 Stirrer Speed : Stirrer speed is the most important parameter, as particle suspension and turbulence levels in the vessel are determined by it. Previous investigators predicted varying effects of speed on  $K_{sl}$ . Studies were conducted for both baffled and unbaffled vessels.

For his system with  $H_t/D_t$  equal to 1.0, Harriot(1) found that mass transfer coefficient was proportional to  $N^{0.5}$  for particles larger than  $100\mu$ . For smaller particle the exponent decreased gradually, and found to be 0.3 for  $15\mu$  particles. The coefficient in unbaffled tanks increased with only 0.3 power of stirrer speed. At lower speeds the coefficients were observed to be higher without

baffles because a higher fraction of the particles were suspended. For the speed that needed for complete suspension in a baffled tank the coefficients were about the same without baffles, under similar operating conditions. However at higher speeds, the more uniform dispersion of particles and greater velocity fluctuations made the coefficients higher with baffles.

According to Barker and Treybal(2), the mass transfer coefficient in unbaffled vessel was observed to be smaller than those in baffled vessel in the region of their study and it was explained by the pattern of fluid motion in an unbaffled tank. It consists of simple rotational flow imposed by turbine, with lower velocity fluctuations than tanks equipped with baffles. Here the mass transfer coefficient was proportional to  $Re^{0.8}$  where  $Re$  is defined as  $(\pi X N X T^2 / \nu)$ .

Sano et al.(3) have carried out experiments, with and without baffles in 20cm diameter vessel, in which the coefficients for baffled vessel were observed to be smaller than that of unbaffled vessel. However they have neglected the difference between these values. And a correlation for mass transfer coefficient proportional to  $N^{0.75}$  was proposed by them.

The conditions selected by Boon-long et al.(4) were such that complete suspension was ensured and there was no solid

breakage, the exponent obtained for Re number, 0.28, was in good agreement with other investigators. Yagi et al.(5), who have studied the mass transfer at higher specific surface area of particles using  $\text{Ca(OH)}_2$ , observed that the effect of speed decreased as surface area increased, while for dilute concentrations the data was fitted well with a correlation  $K_{sl}$  proportional to  $\varepsilon^{0.21}$  where  $\varepsilon$  is power input per unit volume.

1.1.1.2 Particle Size : Barker and Treybal(2) obtained no systematic variation of mass transfer coefficient with particle size. The samples with larger particles exhibited high coefficients, which was attributed to a tendency of these samples to disintegrate rather than any apparent effect of particle size. Harriot(1) reported that, for particles smaller than  $100\mu\text{m}$   $K_{sl}$  varied inversely with size of the particle. However it was almost independent of size for particles larger than  $100\mu\text{m}$ . As the density difference between liquid and solid increased this cut off point increased to  $200\mu\text{m}$ .

Asai et al.(6) have done experiments on  $K_{sl}$  for particle larger than  $100\mu$ . And the results were well correlated with the work of Levins and Glastonebury(7), which was given as  $Sh$  proportional to  $d_p^{0.84}$ . For fine particles  $K_{sl}$  decreased with increase in size of the resin up to  $100\mu\text{m}$ . But the data deviated from Levins et al. correlation reaching the theoretical limiting

correlation for infinite stagnant liquid. This behavior was explained by the diffusivity dependence of  $K_{sl}$ . Separate experiments were carried out for this purpose and observed that  $K_{sl}$  varied with  $2/3$  power of  $D$  for larger particles which agreed with laminar boundary layer theory. On other hand, for fine particles, proportional to  $D$ .

1.1.1.3 Physical Properties of Liquid : The physical properties of the liquid play an important role in solid/liquid mass transfer. Density of liquid phase affects  $K_{sl}$  indirectly and power required for complete suspension of solids also depends on density ( 26). Viscosity of liquid was observed to influence both diffusivity and power input along with Re and Sc numbers.

Barker and Treybal(2) observed no effect of density difference (in the range of below 0.4 and 0.7 & 1.0 gm/cc) between particle and liquid, on mass transfer coefficient. According to Harriot's work(1) density difference has got no effect on  $K_{sl}$  up to 0.4gm/cc. But above this value, it ( $K_{sl}$ ) was proportional to density difference to the power of 0.3-0.4.

The effect of viscosity on  $K_{sl}$  was found to be negligible by Barker et al.(2), which is attributed to the effect of kinematic viscosity on both Sc and Re numbers. Because if Sc number is high, the Reynolds number tends to be low and vice versa. Harriot(1)

observed, with water and methocel solutions having same diffusivity, that  $K_{sl}$  was proportional to  $\nu^{0.22}$  for larger particles and 0.06 for smaller particles. He has also presented the effect of viscosity, that changes with temperature, on  $K_{sl}$ . According to which  $K_{sl}$  was proportional to  $\mu^{-0.37}$  for resin particles of size  $300\mu\text{m}$  and  $\mu^{-0.09}$  for  $15\mu\text{m}$  resin.

1.1.1.4 Tank Size and Design : In the experiments, carried by Barker and Treybal(2), larger vessels yielded smaller  $K_{sl}$  same Reynolds number i.e. for same turbine size. Harriot(1) also observed the similar effect, that for the same power input  $K_{sl}$  with  $T/D_t$  ratio 0.5 were approximately 20% higher than that of  $T/D_t$  equal to 0.25. Since  $K_{sl}$  is proportional to  $\varepsilon^{0.15}$ , which varies with  $T^5$ , more power must be used to get the same  $K_{sl}$  with small impeller diameter. Sano et al.(3) confirmed the above results, using different vessel diameters with same  $T/D_t$ . They observed no effect of vessel size on mass transfer coefficient. Boon-long et al.(4) also on the basis of their experimental results concluded that the effect of vessel size was negligible.

## 1.1.2 AIR AGITATED TANKS

A review of the literature shows that measurement of  $K_{sl}$  in pachuca tanks has not been available so far. Except for the work

of Hallett et al.(11, gas-liquid mass transfer coefficient in pachucas) and shekhar & Evans (12, Fluid flow in pachuca tanks)), there has been very little work on pachuca tanks. However, studies have been carried out on laboratory scale bubble columns on solid/liquid mass transfer by sano et al.(3), Sanger & Deckwer(8) and Jadhav & pangarkar(9,10). Most of the above bubble column investigations employed high superficial gas velocities (up to 0.35m/sec), which are much greater than the velocities being used in pachuca tanks (0.1-0.73cm/sec).

1.1.2.1 Superficial Gas Velocity : Sano et al.(3) had carried out experiments in two different diameter bubble columns without using draft tubes. An increase in Sherwood number was observed with increase in energy input per unit volume which is proportional to  $U_g$ . The correlation obtained from their data :  $K_{sl}$  proportional to  $U_g^{0.25}$ . From their experimental observations the effect of tank size and the method by which flow energy was supplied, were found to be negligible.

The authors, however, did not mention any trend like  $K_{sl}$  to be independent of  $U_g$  at higher gas velocities, which was observed by other investigators. For instance, Sanger & Deckwer(8) indicated an increasing tendency for mass transfer coefficient with  $U_g$  at low gas velocities(<6cm/sec), whereas at higher velocities (i.e.

$>6\text{cm/sec}$ )  $K_{sl}$  values were constant. The reason given by the authors was that at higher gas throughputs only fraction of the energy input dissipated in turbulent eddies of the liquid. They also explained that the constant values of  $K_{sl}$  at higher  $U_g$  was due to a transition from homogeneous to churn turbulent region of flow. It is, however, known that in churn-turbulent region vigorous liquid circulation is set up and this causes an increase in levels of turbulence in liquid phase, which should in turn increase  $K_{sl}$ .

Jadhav & pangarkar(9), have reported observations similar to Sanger and Deckwer. However the levelling of  $K_{sl}$  was observed at slightly higher values of  $U_g$  ( $0.25\text{m/sec}$ ). According to them, the data presented was likely to be above the transition range at the minimum gas velocities and clearly in churn-turbulent situation at higher velocities. The behavior was explained as follows. At high gas velocities a portion of gas may flow as large slugs. These slugs do not contribute significantly to liquid circulation. Further, there may be a chance of some solids to be trapped in the slugs, thereby eliminating contact with the solution.

1.1.2.2 Effect of the Tank Diameter : Sanger & Deckwer(8) hardly found any change in mass transfer coefficient with the liquid volume present in the column, which agreed with the work of sano et al.(3), in which no effect of column diameter was observed. In contrast,

Jadhav & pangarkar(10) showed an increase in  $K_{sl}$  with increase in column diameter, which was contradicting the results of Sano et al.(3) & Sanger et al.(8). Here  $K_{sl}$  was proportional to  $D_t^{0.29}$ . This increase was attributed to higher level of turbulence which is proportional to  $D_t^{0.33}$ .

1.1.2.3 Height to Diameter ratio of the liquid column : The only study on the effect of height to diameter ratio is by Jadhav et al.(9), where the height to diameter ratio of column was varied from 4 to 12 in order to establish its effect on  $K_{sl}$ . It was observed that mass transfer coefficient was independent of height. The above results obtained from Free Air-lift bubble column which are operated at higher superficial gas velocities (<0.35 cm/sec here) and height to diameter ratio much larger than pachuca tanks. Therefore the results of bubble columns may not applicable pachuca tanks directly.

Shekhar & Evans(12,13) carried out extensive velocity measurements in laboratory scale tanks and mathematical modelled flow in industrial-scale pachuca tanks. They reported that, tanks with a large  $H_t/D_t$  ratio and equipped with a draft tube have a near stagnant zone in the lower part of annulus. The stagnant zone is a region of low turbulent kinetic Energy, which is undesirable in terms of mass transfer. An increase in draft tube diameter leads to higher velocities and turbulence levels in the annulus, which should

promote mass transfer. A tank without draft tube is more vigorously agitated than the tanks equipped with draft tubes. Based on the measured and predicted turbulent kinetic energies in both laboratory Scale and industrial-scale pachuca tanks Shekhar and Evans have qualitatively explained the effect of tank design and operating parameters on  $K_{sl}$ .

## 1.2 RESEARCH OBJECTIVE

---

Thus the primary objective of this work has been to study the effect of design and operating parameters of pachuca tanks such as superficial gas velocity, height to diameter ratio of liquid column and draft tube to tank diameter ratio on solid/liquid mass transfer. This is rather important because a survey by Hallett et al.(11) has shown that there is a wide variation in design and operating parameters used in pachucas (Table 1). For example, tank height to diameter ratio vary by a factor 3, superficial gas velocity vary by a factor of more than 7, while cone angle  $30^{\circ}$  to  $64^{\circ}$ . These authors do not report on variation of the draft tube diameter and location of air injecting point. Furthermore no clear guide lines for the selection of such parameters are available. Therefore our experiments may shed light on the design and operating parameters of pachuca tanks used in industry. Finally a preliminary

TABLE 1

Type of Leach	Gold Cyanide				
Tank Height (m)	13.72	15.24	15.24	15.24	15.24
Tank Diameter (m)	4.5	6.86	5.03	6.86	10.72
Height/Diameter	3.05	2.22	3.03	2.22	1.5
Superficial Velocity (cm/sec)	0.73	0.45	0.50	0.19	0.10
Cone Angle (degrees)	60	60	30	60	60
Froude Number ( $Fr \times 10^{10}$ )	4.72	1.62	2	0.29	0.08
Particle Size (µ below 74 µm)	70	45	78	-	75
Bed Weight ( $\times 10^{-3}$ kg)	247.7	775.4	257.0	800.5	1499.2
Airlift	Yes	No	No	No	No

Superficial air velocity = Air flowrate/Tank cross-section area

$$\text{Froude number} = \frac{\text{Superficial air velocity}^2 \times \rho_G}{(\rho_L - \rho_G) g H_t}$$

comparison between the performance of air and mechanically agitated tanks will be made.

## CHAPTER II

### EXPERIMENTAL APPARATUS AND MEASUREMENTS

This investigation was aimed at evaluating the effects of superficial gas velocity, draft tube diameter, tank height and tank design on solid-liquid mass transfer coefficient,  $K_{sl}$ . The air agitated tank was designed so that the design and operating parameters were in the same range as those used in the industry (Table 2). Before that, some experiments were carried out in mechanically agitated tanks to select conditions under which the reaction would be controlled by transport of species from bulk liquid to solid/liquid interface.

In this chapter, the experimental set-up for mechanically and air agitated tanks are discussed, along with calibration of relevant instruments. The procedure for determining  $K_{sl}$  from the experimental data has also been presented. Apart from these, some of the important factors like position of the conductivity probe, draft tube and nozzle inlet and effect of submergence of the draft tube in air agitated tanks are discussed.

#### 2.1 EXPERIMENTAL APPARATUS AND CALIBRATION

##### 2.1.1 Mechanically Agitated Tanks

The experimental setup for mechanical agitation is shown

TABLE 2

Design and Operating parameters used in Industrial  
and Laboratory scale Pachuca tanks

PARAMETERS	INDUSTRY	EXPERIMENT
$H_t / D_t$	1.5 to 3.0	1.5 to 2.5
$D_d / D_t$	approx. 0.1	0.08 to 0.3
$U_g * 10^2$ (m/sec)	0.1 to 0.73	0.18 to 0.73
cone angle	$30^\circ$ to $60^\circ$	$45^\circ$

in Fig. 2.1. The vessel was filled with an aqueous solution to a depth equal to its diameter(12.5cm). The impeller used for agitation was of propeller type, had 3 blades and was 3.8cm in diameter. The impeller was connected to a motor of 1H.P. capacity with a maximum rotational speed of 4000 RPM. To obtain different speeds, a variac was connected to the motor. A voltmeter and an ammeter were used to measure power consumption at different speeds.  $K_{sl}$  was determined by monitoring the conductance of the aqueous solution with time, details of which are given in a later section.

Mechanical Agitator (Stirrer) : For agitation of the solution in the vessel, the stirrer was kept at one third of the height from bottom of the liquid column present. According to the literature available it was the optimum height with respect to both the power consumption and suspension of the particles. This fact, was also confirmed by our experiments. Furthermore, Harriot(1) had observed that  $K_{sl}$  was unaffected by the position of stirrer once all particles were completely suspended.

Calibration of Stirrer : The stirrer speed was calibrated with a STROBOSCOPE and the relevant curve is shown in Fig.2.2.

Constant Temperature Bath : A JULABO FC20 constant temperature bath was used to carry out experiments at  $60^{\circ}\text{C}$ . With this equipment temperature can be maintained between  $0^{\circ}\text{C}$  and  $999^{\circ}\text{C}$  with an accuracy

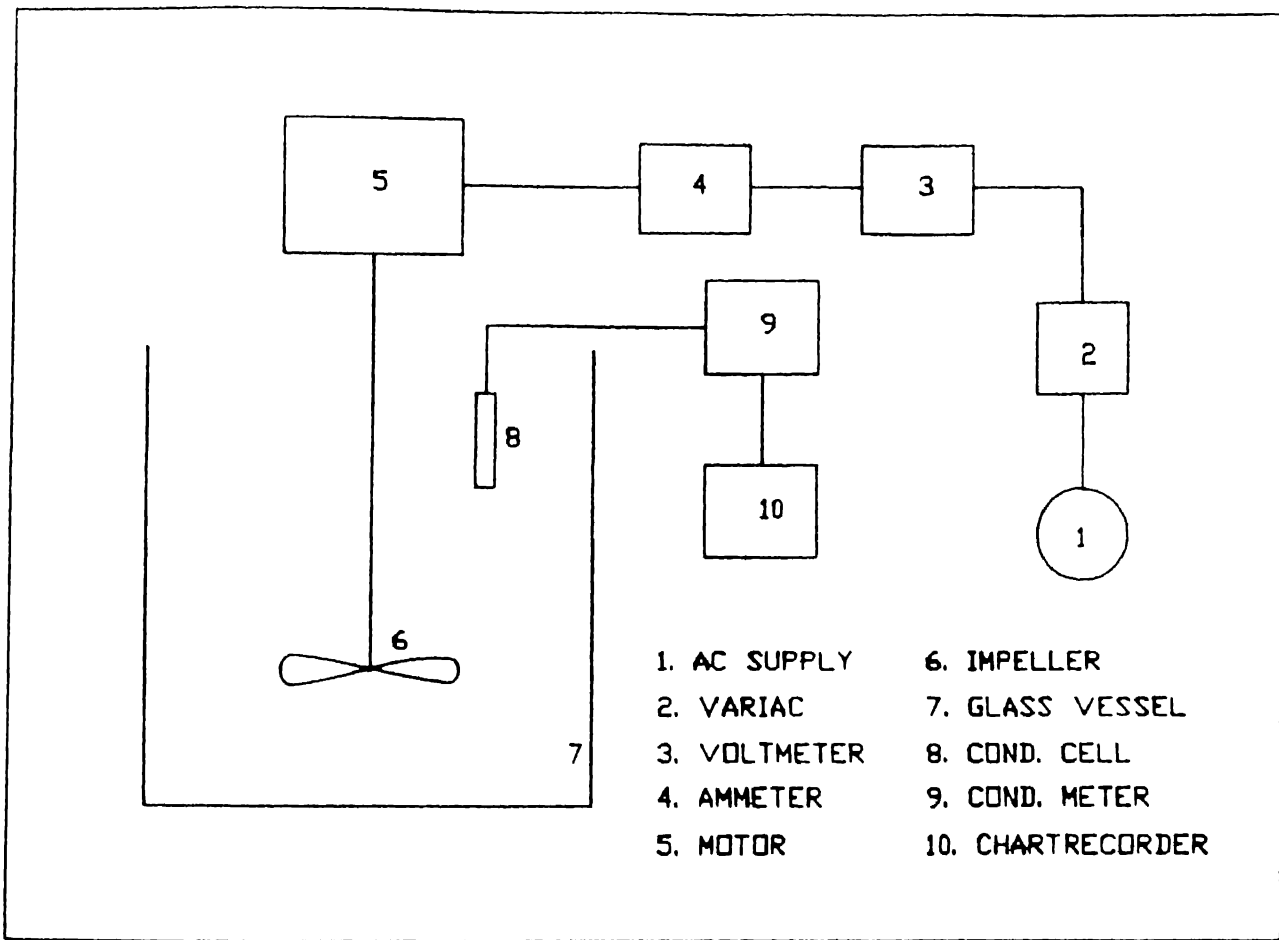


Fig. 2.1 Experimental set-up - Mechanically agitated tank

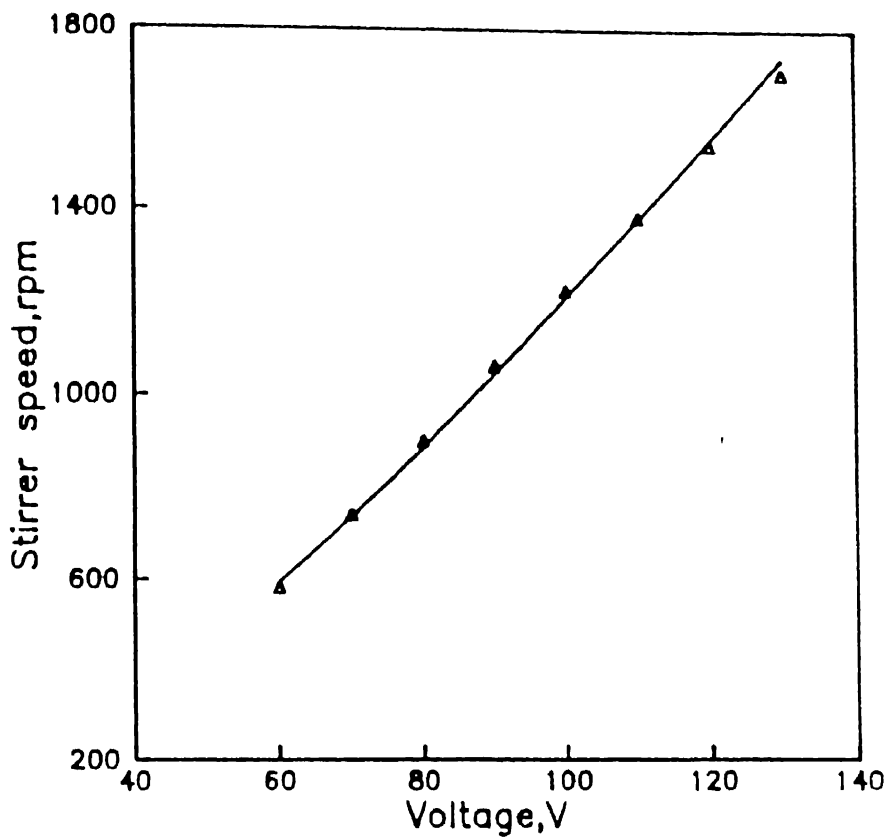


Fig.2.2 Calibration of Mechanical stirrer

of  $0.2^{\circ}\text{C}$ .

#### 2.1.2 Pachuca Tank

Fig. 2.3 depicts a schematic diagram of the Pachuca tank used in our experiments. It consists of a cylindrical tank 15 cm in diameter and 60 cm in height. For the purpose of having a conical bottom, a cone (cone half angle equal to  $45^{\circ}$ ) was placed at the bottom of the tank. This configuration ensured that cones with different angles could be used readily without any modification in the experimental set-up.

Air was supplied to the tank from a compressor through a capillary flowmeter. As mentioned earlier, the draft tubes were placed just above the air injection point, running parallel to the length of the tank. Glass pipes of different diameters and lengths were used as draft tubes. As shown in Fig. 2.3 the draft tube was suspended from the top with the help of a vertical rod. To restrict the movement of the draft tube in the horizontal plane another rod was used to clamp the vertical rod in position. The whole system was placed on an iron structure and the tank was bound from four sides by slotted angles to restrict its movement.

**Calibration of Capillary Flowmeter :** The capillary flowmeters were calibrated using a wet-testmeter and the calibration charts are shown in Fig. 2.4. Furthermore, experiments showed that the

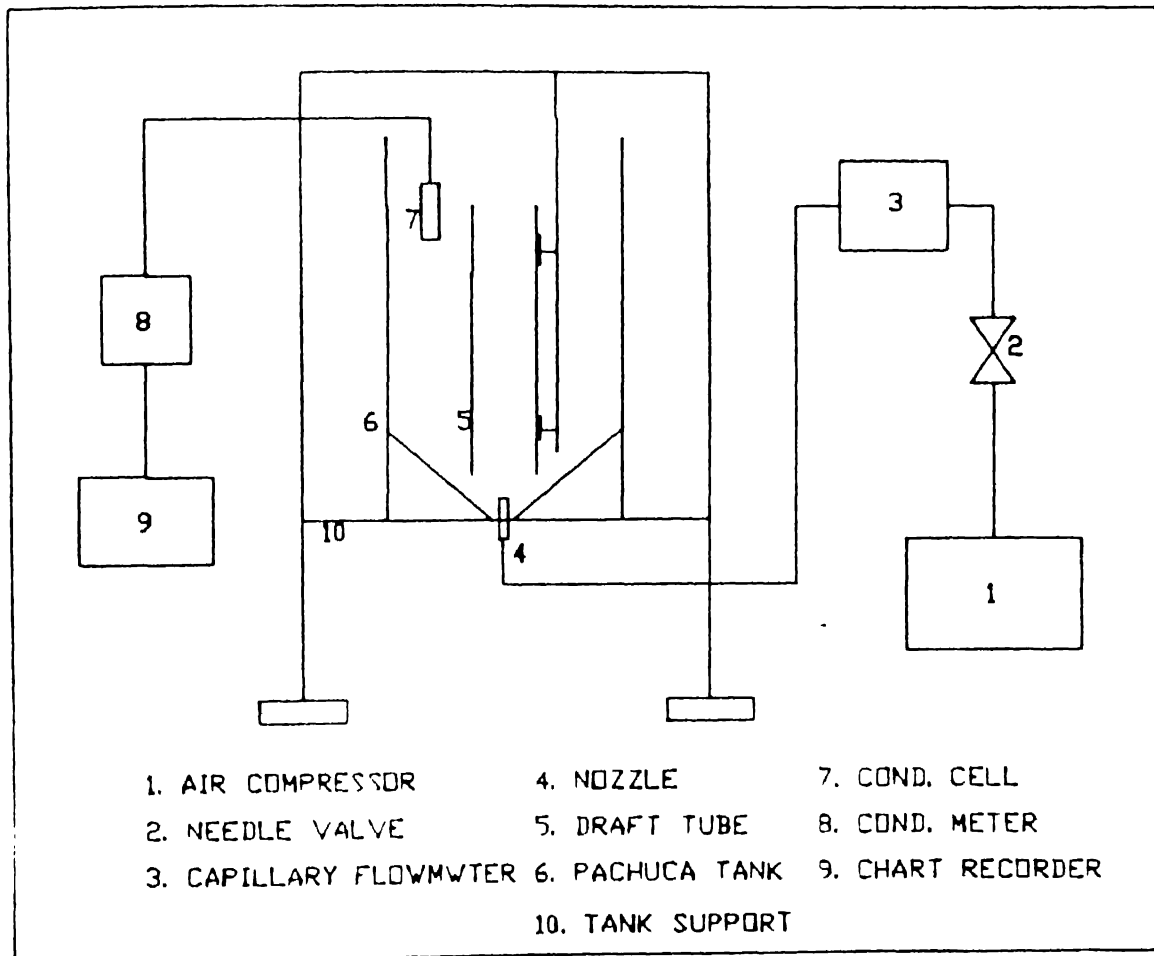


Fig. 2.3 Experimental set-up - Air agitated tank (Pachuca)

correlation curves were largely unaffected by the height of the water column in the laboratory-scale pachuca tank.

## 2.2 CONDUCTIVITY MEASUREMENTS

---

$K_{sl}$  was determined with the help of conductivity measurements. A SICO-GLOBAL conductivity meter (DCM1000) was used to measure the conductivity of the solution. The conductivity cell consisted of two platinum electrodes on which a thin layer of platinum chloride was coated. This instrument measures the resistance of the fluid between these electrodes and directly gives the specific conductance.

Calibration of Conductivity Cell : The conductivity cell was calibrated with aqueous KCl solution. Solutions of different concentrations were prepared to cross check calibration. The cell was tuned with a 0.1N solution. Unfortunately, for solutions of higher concentration, such as 1N, the meter reading was more than the theoretical value. An opposite effect was observed for lower concentrations ie. 0.001N solution. Hence, a multiplying factor was defined for concentrations ranging from 0.001N to 1.0N. This is the ratio of theoretical value to the actual value. Fig.2.5(a) shows the graph between the multiplying factor and the concentration of the aqueous solution. Similar trend was obtained for HCl and is

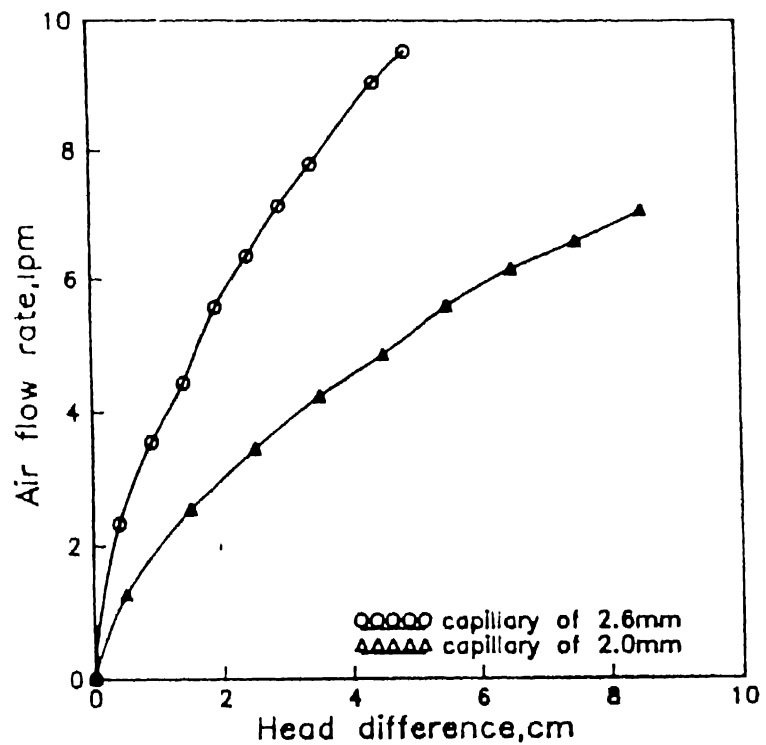


Fig. 2.4 Calibration of Capillary flowmeters

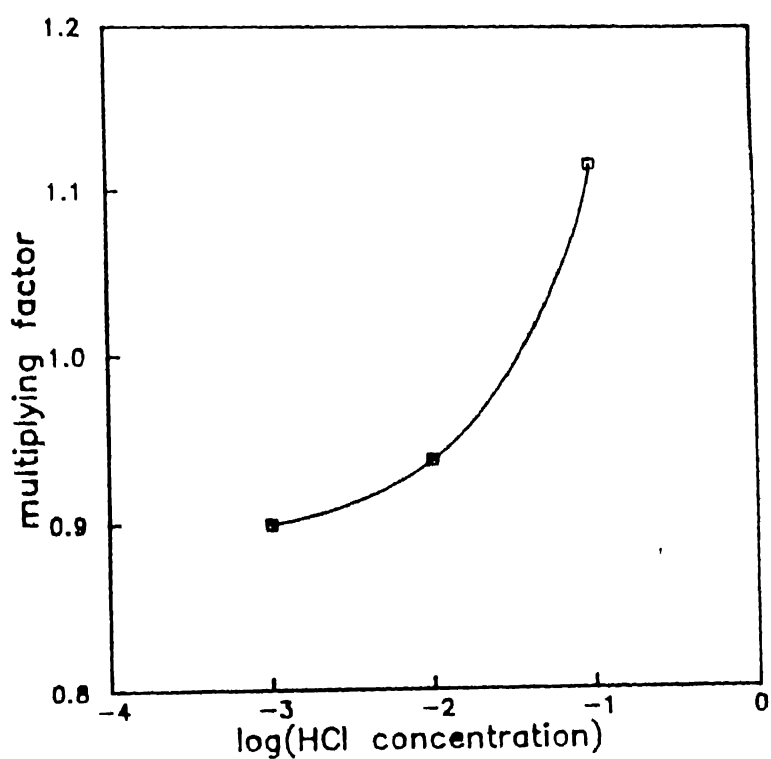
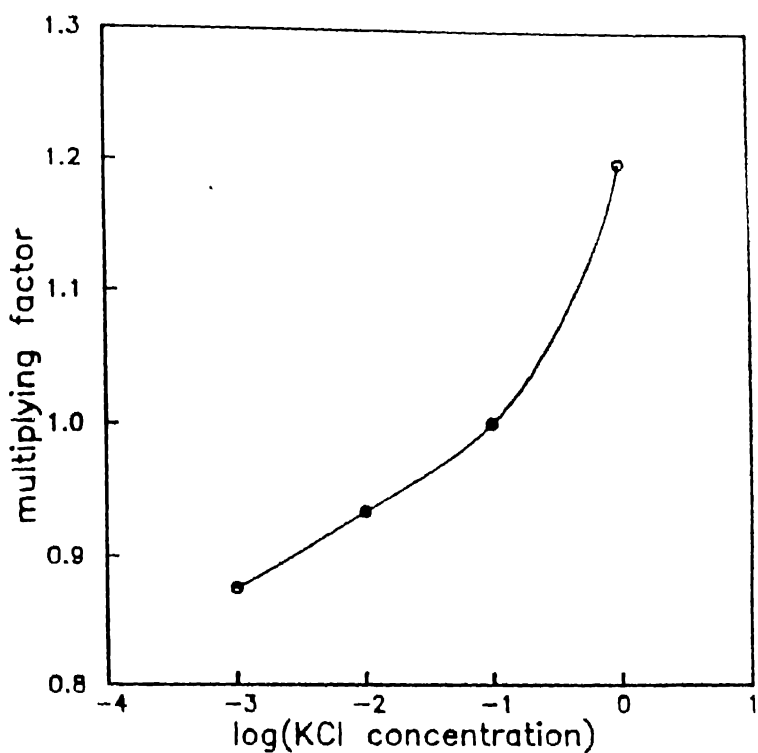


Fig. 2.5 Calibration of conductivity cell

shown in Fig. 2.5(b).

**Conductivity Cell Response Rate :** Any electronics instrument takes a finite time to attain steady state output. The response lag of the instrument may or may not be negligibly small. This period of time is not important for steady state measurements, but it may be relevant in transient measurements. Since the conductivity of the solution is measured as a function of time in this study it was essential to check the response rate of the cell. To measure the response rate, the conductivity cell, after its calibration was transferred to a 0.01N KCl solution and the change in output of conductivity cell with time was recorded on chart recorder. Fig. 2.6 & 2.7 compare the response under these conditions with those observed during our actual runs with ion-exchanger resin. It is evident that the response lag of the conductivity meter would have no bearing on our experimental results.

## 2.3 EXPERIMENTAL MEASUREMENTS

### 2.3.1 Measurement of the mass transfer coefficient - Theory

Ion exchange resins have been used extensively to measure mass transfer coefficient in agitated vessels (1, 3, 6, 8 and 14). In our experiments Styrene DVB 225  $H^+$  type cation exchanger resin was used in an aqueous KCl solution and the exchange reaction

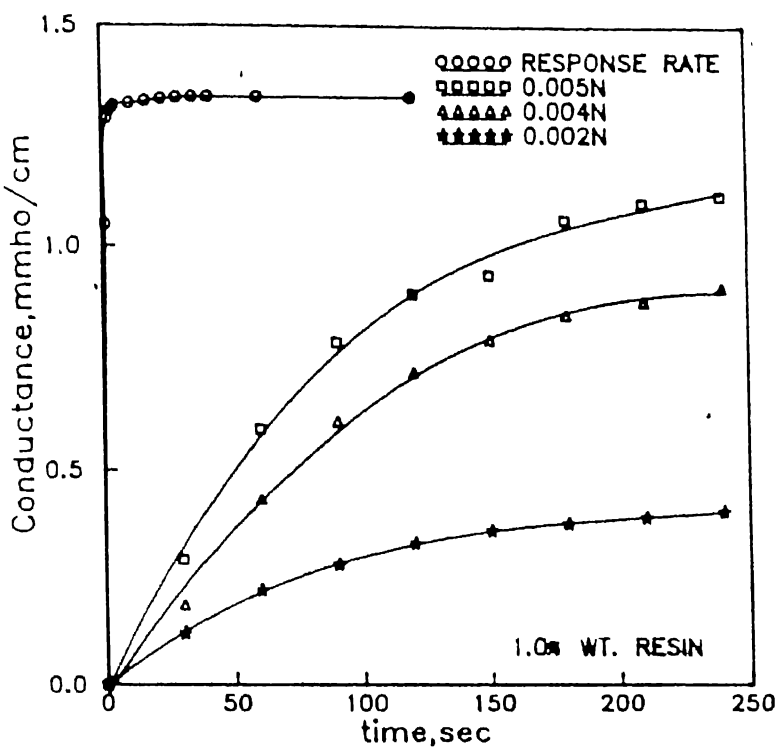


Fig. 2.6 Typical chart recorder traces with different concentrations of aqueous solution

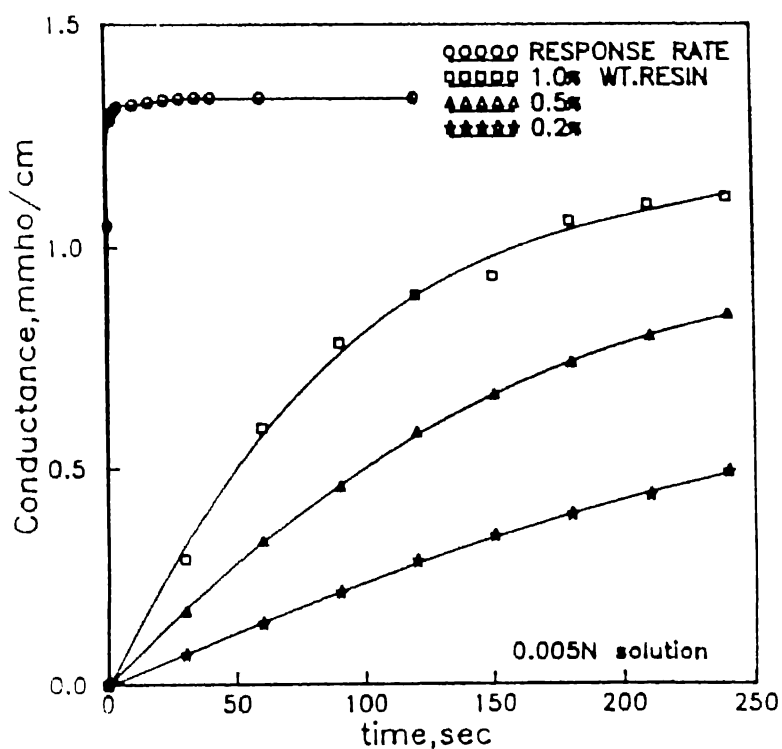
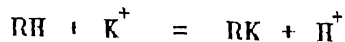


Fig. 2.7 Typical chart recorder traces with different percentages of resin

proceeds as follows:



As the reaction progresses, the  $K^+$  are gradually replaced with  $H^+$  with a concomitant increase in the electrical conductivity of the solution. Consequently, a plot of  $K^+$  concentration with time will yield  $K_{sl}$ :

$$- (dY_b / dt) \times C_o \times V = K_{sl} \times A \times (Y_b - Y_i) \times C_o \quad \text{--- (2.1)}$$

where

$Y_b$  = mole fraction of  $K^+$  in the bulk solution

$Y_i$  = mole fraction of  $K^+$  at the solution-resin interface

$C_o$  = initial concentration of  $K^+$

$V$  = volume of solution

and  $A$  = Total surface area of the resin

$$= 6.0 \times W / (\rho \times d_p)$$

Here,  $W$ ,  $\rho$  and  $d_p$  are weight, density and diameter respectively of the particles.

The other kinetic steps in the exchange reaction are diffusion through the pores in the resin and exchange reaction. To ensure that  $K_{sl}$  corresponds to the condition where external mass transport is the rate controlling step, equation 1 is evaluated at  $t=0$ :

$$K_{sl} = - (V/A) \times (dY_b / dt)_{t=0} \quad \text{--- (2.2)}$$

Since it was not possible to continuously monitor the concentration of  $K^+$  in solution, the solution conductivity was measured as a function of time.  $K_{sl}$  can be evaluated from conductivity data if the relationship between  $Y_b$  and solution conductivity can be established. This is the subject of the following section.

### 2.3.2 Correlation Between $Y_b$ and Solution Conductivity

A 0.002N KCl solution was taken in a beaker and both pH and conductivity values were recorded. This solution was gradually diluted by adding 0.002N HCl in steps. At the end of each step, pH and conductivity were measured. To check the accuracy of the above experiments, a similar experiment was carried out with a 0.002N HCl solution that was diluted in steps with 0.002 N KCl. Fig. 2.8 depicts the conductivity versus pH curve for the above experiments and, as expected, curves for the two different starting solutions are in agreement with each other. Since,

$$pH = -\log [H^+]$$

$$Y_b = \{ n(K^+) / [ n(K^+) + n(H^+) ] \}$$

where  $n(K^+)$  = No. of moles of  $K^+$  and  $n(H^+)$  = No. of moles of  $H^+$

Fig. 2.8 was used to determine the correlation between solution conductivity and  $Y_b$  (depicted in Fig. 2.9)

$$\sigma = -0.548 \times Y_b + 0.842 \quad \text{--- for 0.002N}$$

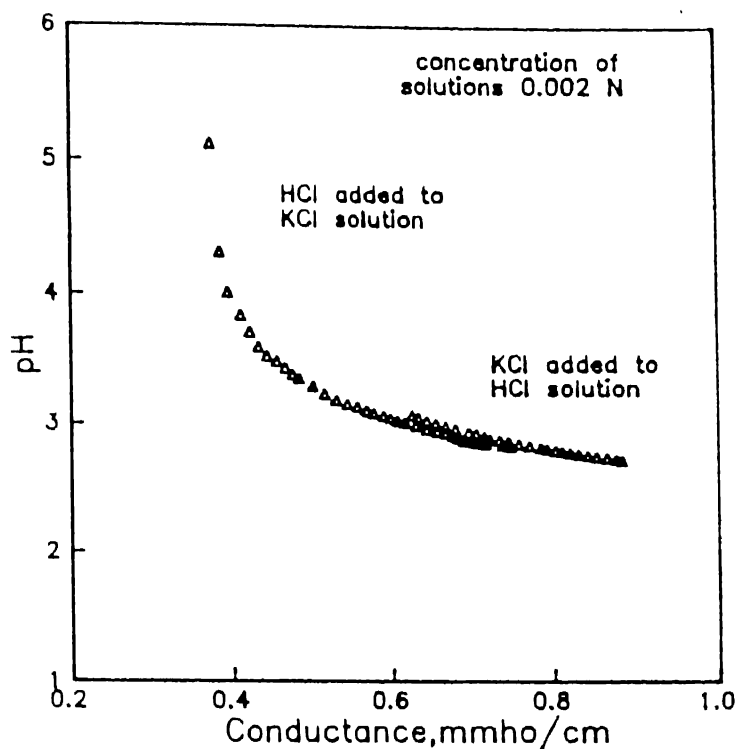


Fig. 2.8 A plot between pH and conductance

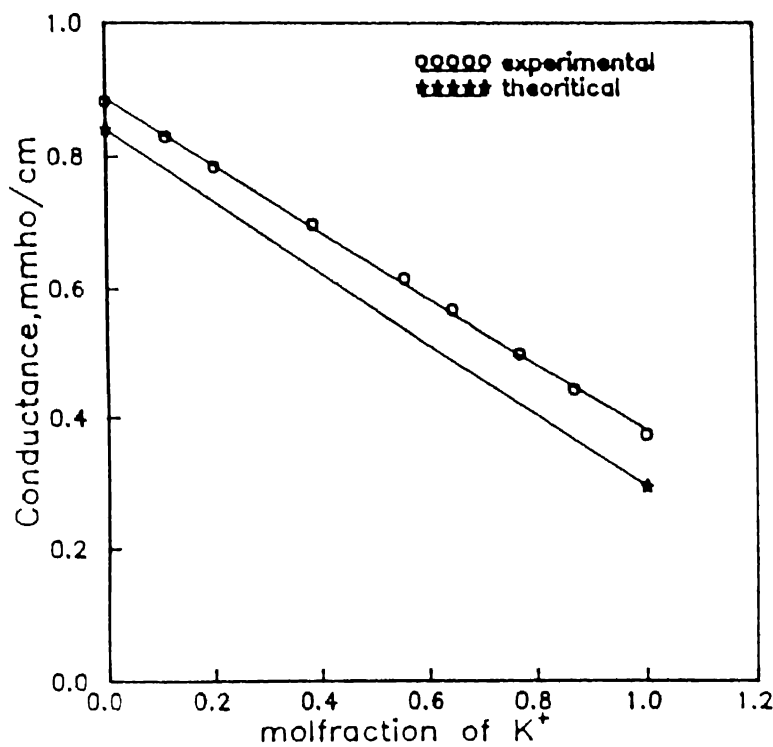


Fig. 2.9 Correlation between molfraction of  $K^+$  and conductance

Similar correlations were obtained for different concentrations of solutions and a general correlation equation is given as:

$$\sigma = M \times Y_b + \text{constant}$$

Therefore  $K_{sl}$  was evaluated from the following equation:

$$K_{sl} = - (V/A) (1/M) (d\sigma/dt)_{t=0} \quad \text{--- (2.3)}$$

## 2.4 EXPERIMENTAL CONDITIONS

---

### Starting Solution Concentration

In the initial stages of the exchange reaction, two kinetic steps are expected to be controlling the rate of dissolution: (a) external mass transport and (b) reaction at the outer surface of the resin. To ensure that external mass transfer is the rate controlling step, concentration of KCl should be very small. In fact, most investigators have used starting solutions of the order 0.001 N containing between 0.05 to 1.5 wt. % of resin (1, 3, 6 and 8). Experimental verification of these numbers have not been reported, except Harriot (1) and Yagi et al.(5). Whereas Sano et al.(3) checked the veracity of their starting concentration using Helffreich's equation(15):

$$\frac{x \times D \times \delta}{c \times D \times r_p} (5 + 2 \times \alpha_B^A)$$

If the above expression is  $\gg 1$ , then the exchange reaction is controlled by external mass transport. However, the above expression was derived for: (a) infinite solution volume, (b) complete conversion and (c) counter ions of equal mobility. However, these conditions do not exist in our system.

Experiments were, therefore, carried out in a mechanically agitated tank at an RPM of 1200. Other details of this tank have been discussed in a previous section of this chapter. KCl concentration in the starting solution was varied from 0.0005 to 0.005 N. The amount of resin in each starting solution was varied in the range of 0.1 to 1.0 wt. %. Fig. 2.10 shows that  $K_{sl}$  is almost independent of concentration, barring the values at 0.001 N. This was expected since the turbulence within the tank is a function of rpm only which, in turn, affects  $K_{sl}$ . Also, the resin concentration, up to 0.5wt. %, did not have a significant effect on  $K_{sl}$ ; the bandwidth being approximately 20%. A similar trend was reported when experiments were repeated at an rpm of 1500 (Fig. 2.11). More importantly, a comparison of Figs. 2.10 & 2.11 clearly showed that  $K_{sl}$  increased with rpm which is possible when the reaction is controlled by external mass transport. Based on the above results, starting concentration of 0.002 N KCl containing 0.2% wt. of resin was selected for our experiments.

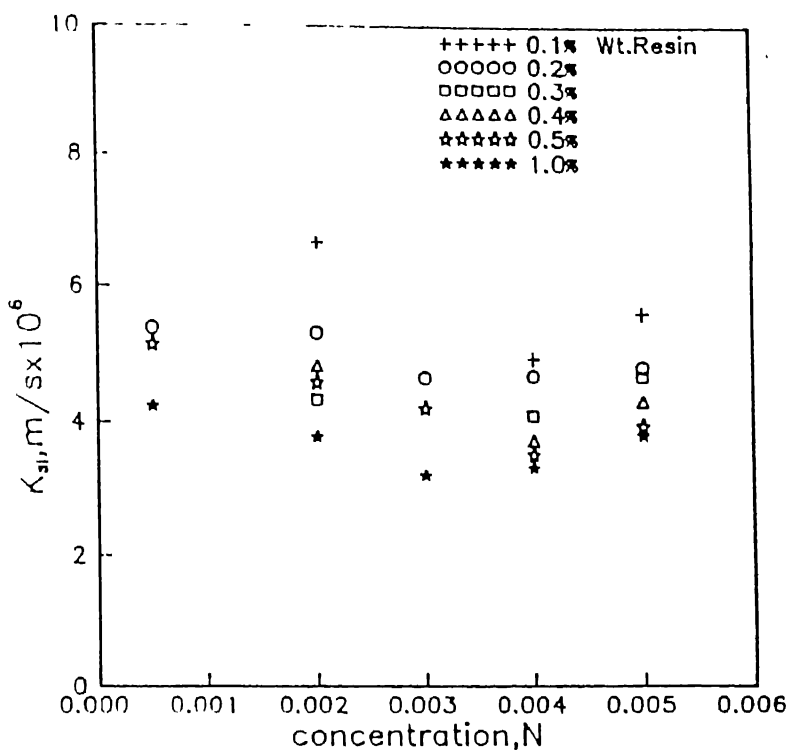


Fig.2.10 Effect of the concentration of aqueous solution on  $K_{sl}$  at 1200rpm

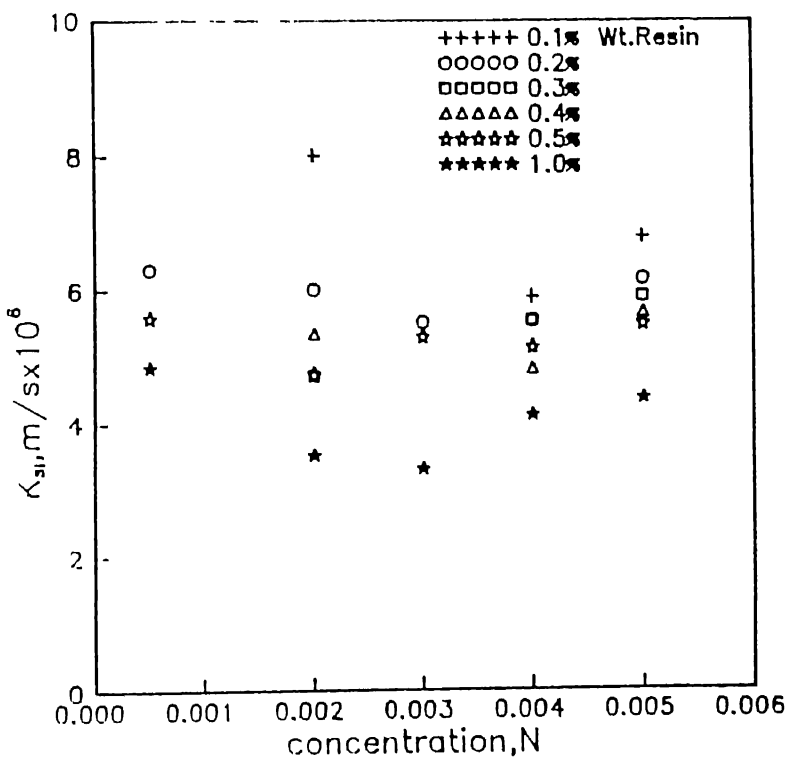


Fig.2.11 Effect of the concentration of aqueous solution on  $K_{sl}$  at 1500rpm

To further confirm that the selected KCl concentration and wt. % resin would ensure that the exchange reaction was controlled by external mass transport, the effect of temperature on  $K_{sl}$  was determined. Experiments were carried out by placing the mechanically agitated tank inside a JULABO type constant temperature bath. Temperature was varied from 10 to 50<sup>o</sup>C. It is well known that the activation energy for diffusion through solution is usually of the order of 5.0 Kcal/mol or less. On the other hand, the activation energy for a chemically controlled dissolution process is in the range of 10 to 25 Kcal/mole. From Fig.2.12 which is a plot of  $\ln K_{sl}$  vs  $1/T$ , the activation energy for the initial stages of the reaction was calculated to be 2.6Kcal/mole. This clearly justified our choice of 0.002 N KCl solution containing 0.2wt. % resin for determining  $K_{sl}$  in our experiments. Furthermore, the water temperature along with room temperature had been observed to vary by a magnitude of about 7 to 10<sup>o</sup>C due to the seasonal variation. Therefore, a correlation between  $K_{sl}$  and temperature obtained from Fig.2.13 was used to present all our data at a single temperature. This correlation is:

$$K_{sl} = 2.076 + 0.1438 \times T - 0.0012 \times T^2$$

## 2.5 EXPERIMENTAL PROCEDURE

---

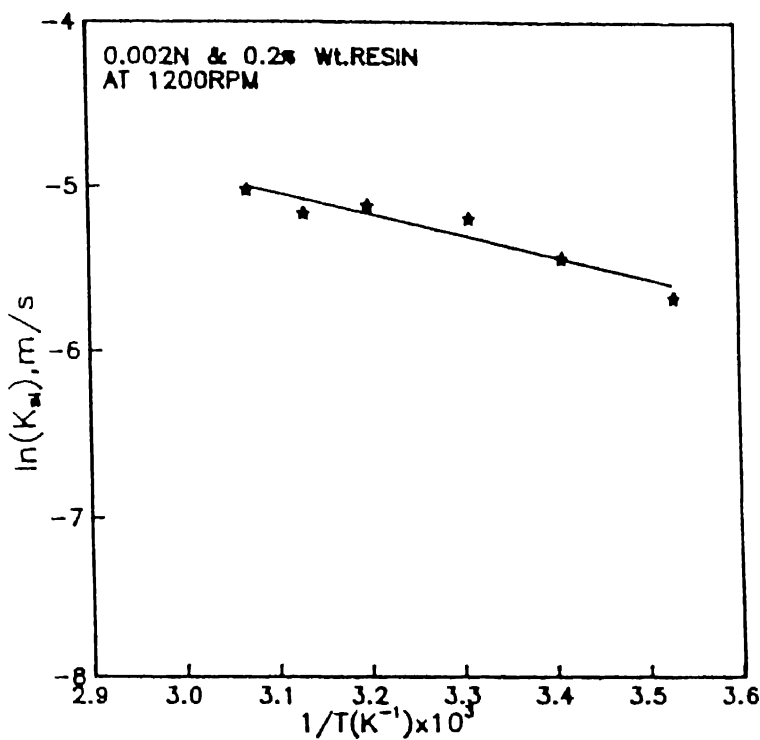


Fig. 2.12 Typical activation energy curve for ion exchange reaction

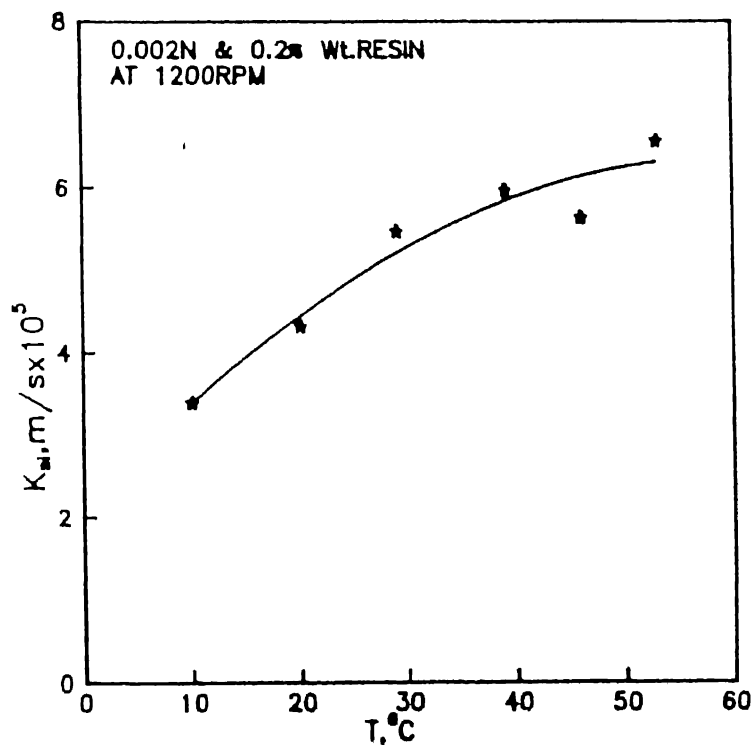


Fig. 2.13 Effect of temperature on  $K_s$

### 2.5.1 Superficial Gas Velocity

---

The superficial gas velocity was defined as the ratio of the volumetric gas flow rate to the cross-sectional area of the tank. In our experiments, the superficial gas velocity was varied from 0.15cm/sec to 0.75cm/sec, which is in the same range as those used in industrial scale pachuca tanks(11).

### 2.5.2 Position of Conductivity Probe

---

The position of electrode is an important parameter because it was observed that mass transfer coefficient varied with the position of the electrode in the tank. Fukuma and coworkers(16) carried out experiments with a number of electrodes placed in the solution at the top of the tank. They observed that  $K_{sl}$  values near the wall region were about 20% smaller than those of the core region. This was attributed to suppression of turbulence near the wall. However, the variation of  $K_{sl}$  with radial position was small except in the region close to the wall.

The electrode was positioned 4 cm below the water level and 4 cm away from the wall to avoid the low turbulent region beside the wall. Before starting an experiment the electrode was allowed to stabilize for constant fluid flow conditions for about 15 to 20 minutes in agitation condition. When a steady state condition with constant conductivity reading was obtained, solids were introduced

in the aqueous solution and actual run was carried out.

#### 2.5.3 Position of the Nozzle and the Draft Tube

---

Experiments were performed to examine the effect of design and operating parameters on  $K_{sl}$  for the condition of full suspension of resin particles in the solution. So it was very essential to fix the positions of draft tube and air inlet such that the particles were fully suspended. This was decided by observing the particles settling near the bottom.

First, the air inlet was fixed at a height 30 mm from the bottom of the cone. And then the draft tube position was varied from top to bottom to locate the position where all the particles were suspended. Above this position the particles were not suspended effectively. And below this the liquid circulation was obstructed by draft tube due to decrease in gap between the draft tube and the cone and settling of particles was observed. By trial and error method, the draft tubes were finally fixed at a height of 5 mm from the bottom of the tank for  $D_d/D_t$  equal to 0.08 and 0.18. It was also observed that the position of the bigger draft tube ( $D_d/D_t$  equal to 0.3) was a bit higher than that of smaller draft tubes of  $D_d/D_t$  0.08 and 0.18.

After selecting the position of the draft tubes the position of the air inlet was varied from 4 mm to 30 mm from the

tank bottom and negligible effect was observed on suspension of particles. Finally a position of 12 mm was fixed for air inlet, keeping the draft tubes in their respective positions.

#### 2.5.4 Effect of Submergence of the Draft Tube

---

Shekhar and Evans(12) have studied the effect of submergence, i.e. the distance between the draft tube top and the liquid surface, on the flow profile. Axial velocity measurements, as reported by them, on the top section of the tank showed that both the mean and fluctuating velocities decreased with decrease in submergence. This, in turn, implies lower liquid flow rate and turbulence levels within the tank. Therefore, it is clearly disadvantageous to operate a pachuca tank with liquid surface at the same level or below the draft tube top. Actually there will be an optimum submergence for a given configuration. The works of Koide and coworkers(17) have shown that higher submergence would lead to a reduction in circulating liquid flow rate. So the effect of submergence can be taken care of by keeping the top of draft tube at approximately 3 to 4 cm below the water level.

#### 2.5.5 Configuration of Free Airlift(FAL) Tank

---

Since Free air-lift tanks are also important from industrial point of view, it would be interesting to compare their performance with that of FCC pachucas. Experiments were carried out

by keeping the liquid column height same for both the FAL and FCC.

Koide et al.(18) reported that solid particles were distributed more uniformly in the column with draft tube. The critical gas velocity for a tank equipped with draft tube was observed to be much smaller than that without a draft tube, where the critical velocity was defined as one at which all particles will be suspended in the column.

Since the same problem of particle suspension was observed in FAL, it was not possible to suspend resin particles at velocities that were used in pachucas with draft tube. To overcome this problem a special arrangement(configuration) was used by which particles were kept suspended (Fig.2.14). By keeping a constant air flow rate in side-tubes, the air flow rate was varied from 0.15 to 0.75 cm/sec through the centre tube.

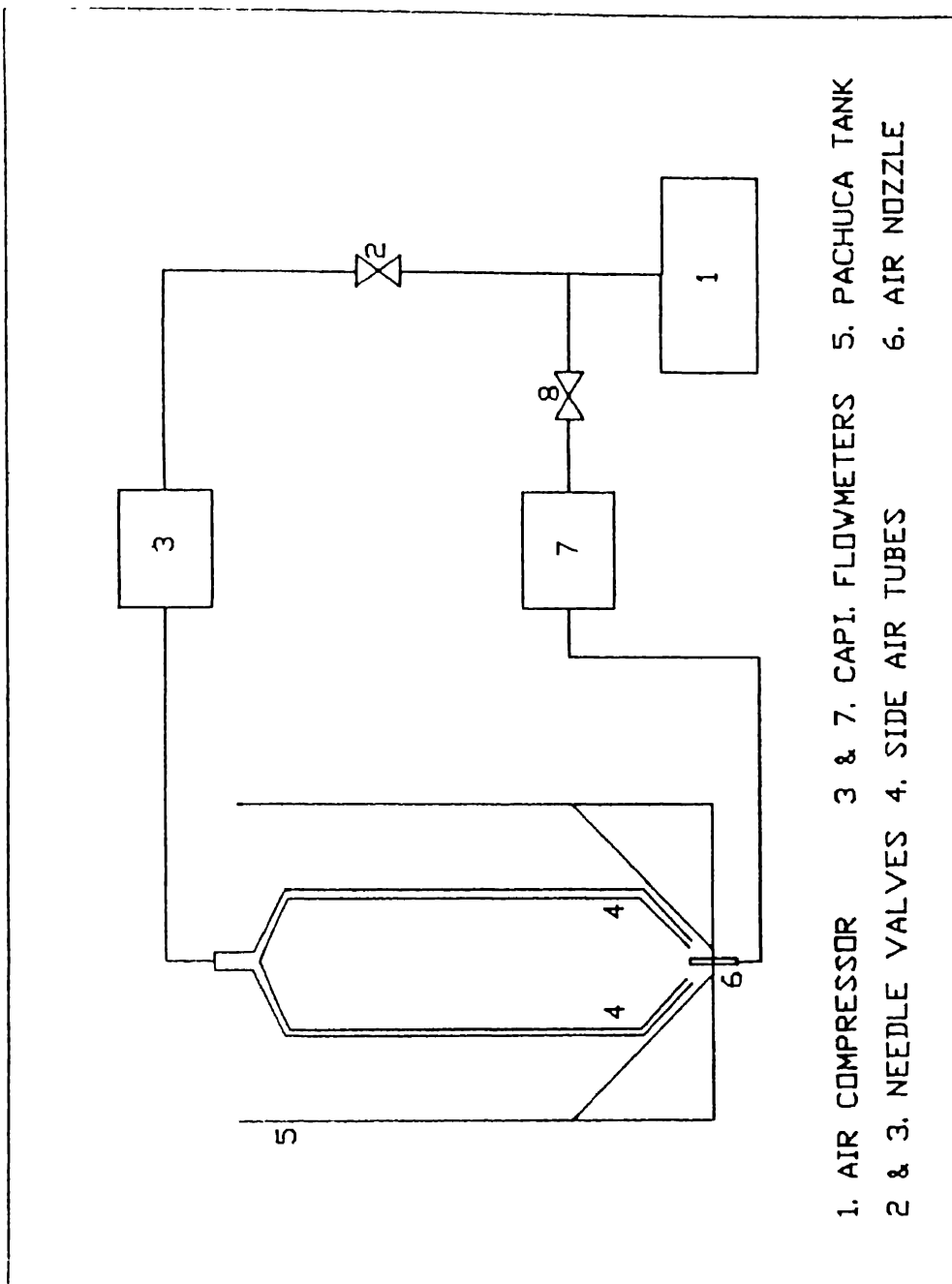


Fig. 2.14 Experimental set-up for Free Air-lift tanks

## CHAPTER III

### RESULTS AND DISCUSSION

As mentioned in the previous chapter, leaching experiments were carried out both in the mechanically agitated and air agitated pachuca tanks. The primary aim of the experiments in the mechanically agitated tanks was to identify the turbulent conditions under which the dissolution process was controlled by external mass transport, that is the mass transfer of reacting species from the bulk liquid phase to the solid/liquid interface. A preliminary comparison of power consumption in the two types of tanks was also to be made. In this chapter first the results of experiments using mechanically agitated tanks are presented. This is followed by the results of the pachuca tanks.

#### 3.1 MECHANICALLY AGITATED TANKS

The parameters and their ranges that have been covered in mechanically agitated tanks is given in Table 3. The effect of these parameters on the rate of dissolution is given below.

##### 3.1.1 Effect of Stirrer Speed on $K_{sl}$

The effect of stirrer speed was studied varying the speed from 600 to 1650 RPM. Two cases, with 0.2 and 0.5 weight % resin in

TABLE 3

RANGES OF DESIGN AND OPERATING PARAMETERS STUDIED

MECHANICALLY AGITATED TANKS

(TANK DIAMETER 0.125M, H/D=1.0, D/T=3.3 & B/H=0.333)

PARAMETER	RANGE
STIRRER SPEED	600 TO 1650RPM
CONCENTRATION	$5.0 \times 10^{-4}$ TO $5.0 \times 10^{-3}$ N
PHASE RATIO	0.1 TO 1.0 % BY WEIGHT
TEMPERATURE	10° TO 55° C
BAFFLES	WITH & WITHOUT
PARTICLE SIZE	0.295 TO 0.785MM

AIR AGITATED TANKS (DIAMETER OF THE TANK 0.15M)

TYPE OF COLUMN	D <sub>d</sub> /D <sub>t</sub>	H <sub>t</sub> /D <sub>t</sub>	U <sub>g</sub> (cm/s)
FULL CENTER COLUMN	0.08	1.5	0.18
	0.18		0.365
	0.30	2.0	0.55
STUB COLUMN TYPE	0.18	2.5	0.73
FREE AIR-LIFT			

a solution of concentration 0.002 N KCl have been studied. Fig.3.1 shows the effect of stirrer speed on mass transfer coefficient,  $K_{sl}$ . It was observed that  $K_{sl}$  increased with the increase in stirrer speed. It can also be seen that the slope of the curve is decreasing as the speed increases from 600 to 1650 RPM. This trend may be explained as: it was observed that at 600rpm resin particles are not fully suspended in the solution. However, at 900rpm almost all particles are in suspension.

Once all the particles were suspended the only influencing factor will be turbulence, which decreases the thickness of mass transfer boundary layer around the particle and enhances the dissolution rate. But as the thickness of the layer decreases, it becomes difficult to decrease it further. And finally, it cannot be decreased beyond a point known as limiting boundary layer thickness (Sohn et al.(19)). In fact, that may be the reason for the decrease in slope of the curve and then a tendency towards a plateau-region in the figure. Sohn & wadsworth(19) suggested that diffusion boundary layer in unstirred condition is approximately 0.05cm, diminishing to around 0.001cm under the condition of violent agitation.

### 3.1.2 Effect of Baffles on $K_{sl}$

Experiments were repeated for 0.002 N solution and 0.2wt.%

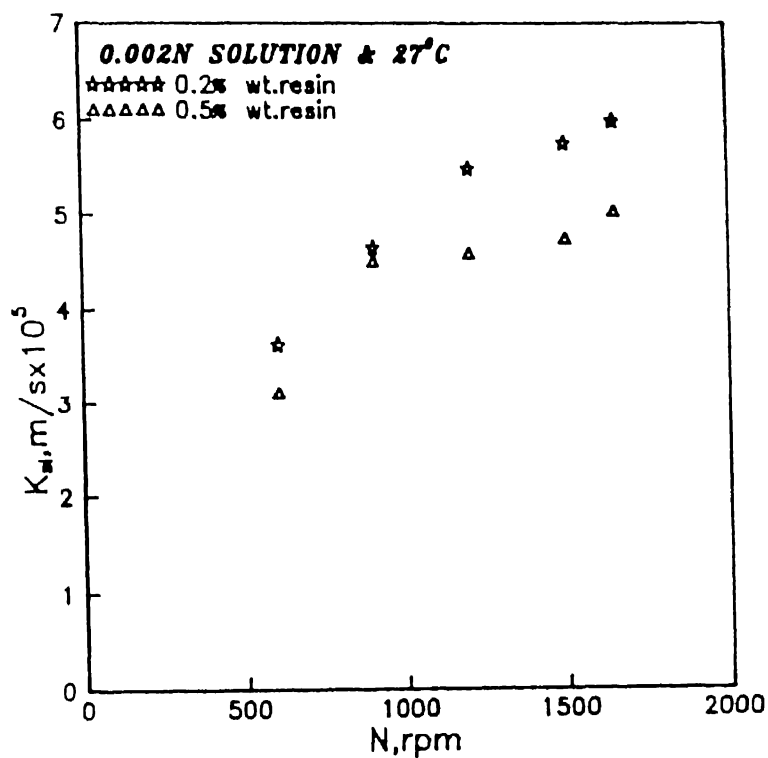


Fig. 3.1 Effect of stirrer speed on  $K_{st}$

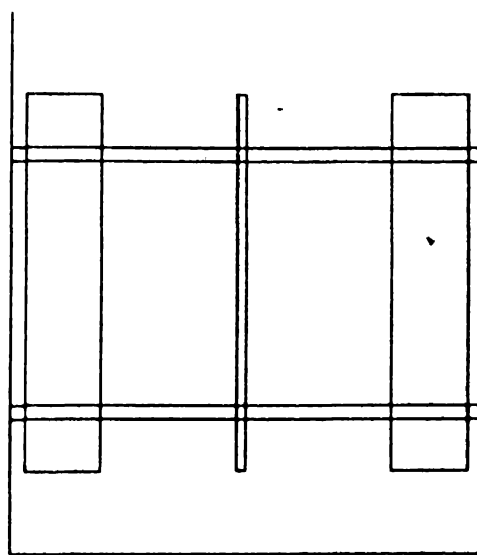
of resin, using baffles. The vessel was equipped with four symmetrically located baffles whose width is 15% of the tank diameter. These baffles are made of Al sheet, 1.5 mm thick, fixed in two perspex rings of 8 mm width. The baffles were positioned 2 cm above the bottom of vessel and 4 mm away from the wall, to eliminate the settling of resin particles or dead pockets (fig.3.2).

The effect of baffles is shown in Fig.3.3.

It was observed that at 600 RPM,  $K_{sl}$  for baffled tank was lower than that of the unbaffled tank. However opposite effect was observed above 900 RPM. This observation was in conformity with the measurements of Harriot(1), who found a similar trend for his system. He explained that at lower speeds a higher fraction of solids were suspended in the absence of baffles and hence  $K_{sl}$  was higher in this configuration. At higher speeds the more uniform distribution of particles and greater velocity fluctuations made coefficients greater for baffled tank. This explanation may be valid in our case also, as it was observed that at lower speeds more solids settled in the presence of baffles. At higher speeds particles were observed to be suspended for both with and without baffles cases. But as mentioned by Harriot, due to the presence of baffles the velocity fluctuations increase and the vortex that was observed in unbaffled tank was not seen here.



BAFFLES



ARRANGEMENT OF BAFFLES

Fig.3.2 Experimental set up for Baffled tank

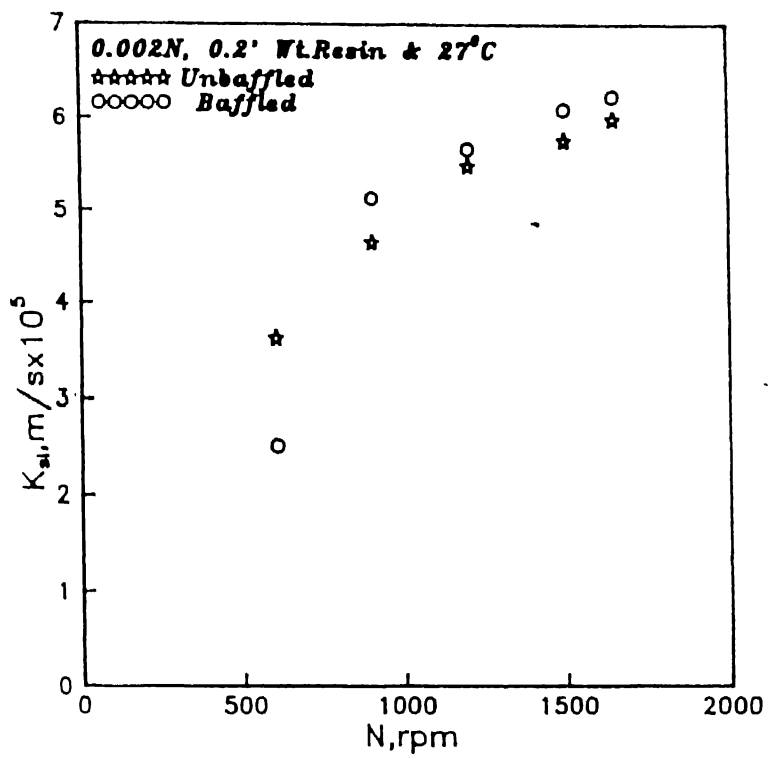


Fig. 3.3 Effect of Baffles on  $K_{sl}$

### 3.1.3 Effect of Particle Size on $K_{sl}$

Experiments were carried out with different sizes of resin. Resin was sieved to different size fractions and the particle distribution was studied using an optical microscope. The particle size varied from 0.23 to 0.85mm. The effect of particle size on  $K_{sl}$  is shown in Fig.3.4. It is clearly seen that the mass transfer coefficient is not significantly affected by the resin size in the range of 0.23 to 0.85 mm.

Harriot(1) also found similar trend for variation of  $K_{sl}$  with particle size. He carried out experiments varying density difference (between solids and liquid) up to 1.0gm/cc. It was observed that the effect of particle size on  $K_{sl}$  changes with the variance in density difference. For a density difference equal to 0.3gm/cc and particle size greater than  $100\mu\text{m}$   $K_{sl}$  was reported to be independent of particle size. Since in our case the density of resin is 1.33gm/cc, and the resin sizes used are much above  $200\mu\text{m}$ , the result obtained can be justified.

### 3.1.4 Correlation Between $K_{sl}$ and Energy Input

A correlation was obtained for the data of 0.002 N solution with varied percentage of resin. From this correlation  $K_{sl}$  is observed to be varied with 0.408 power of energy input per unit volume.

CENTRAL LIBRARY  
I.I.T., KANPUR

Ref. No. A.118182

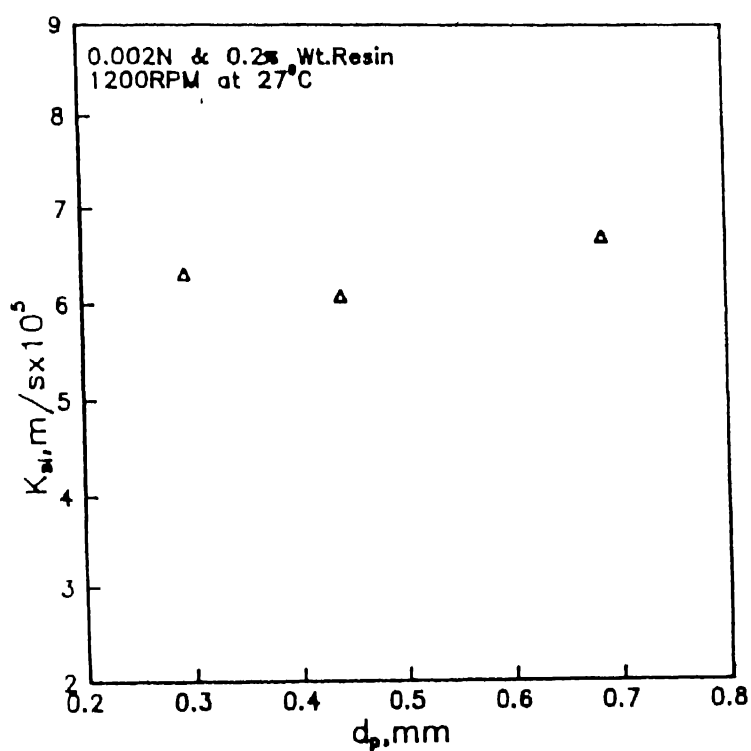


Fig. 3.4 Effect of Particle size on  $K_{sl}$

$$K_{sl} = 1.62 (\varepsilon)^{0.408} (\text{wt. \% resin})^{-0.276} \text{ (unbaffled)}$$

Fig.3.5 shows a plot between measured and correlated values of  $K_{sl}$  in unbaffled tank.

For baffled tanks the regression was obtained for the data of 0.002 N solution concentration and 0.2 wt. % resin only. The equation of correlation is,

$$K_{sl} = 0.0737 \varepsilon^{0.639} \text{ (baffled)}$$

Here  $\varepsilon$  is the energy input per unit volume of the liquid and was calculated from the readings given by the voltmeter and ammeter connected in the circuit. Investigators like Harriot(1) and Sano et al.(3) had calculated the power consumption using the empirical relationship given by Rushton et al.(18), which is given below:

$$\varepsilon = (P \times N^3 \times T^5 \times \rho/V)$$

where  $P$  is the power number that depends on design and operating parameters of the tank being used. The other parameters are,  $N$  is the stirrer speed,  $T$  is the diameter of stirrer and,  $\rho$  and  $V$  represent the density and volume of solution respectively. This expression is applicable only to the tanks equipped with baffles. For unbaffled tanks a correction factor must be used to calculate power input. But for our experimental set up the power calculated using Rustion's equation was observed to be much less than the actual power consumption obtained by the product of voltage and

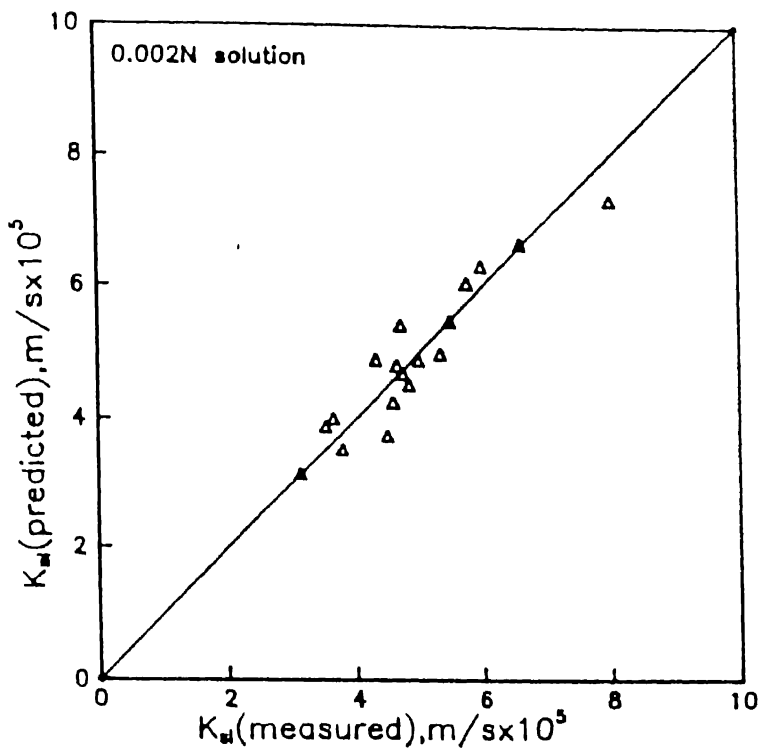


Fig. 3.5 Comparison between measured and predicted values of  $K_{sl}$   
(unbaffled condition)

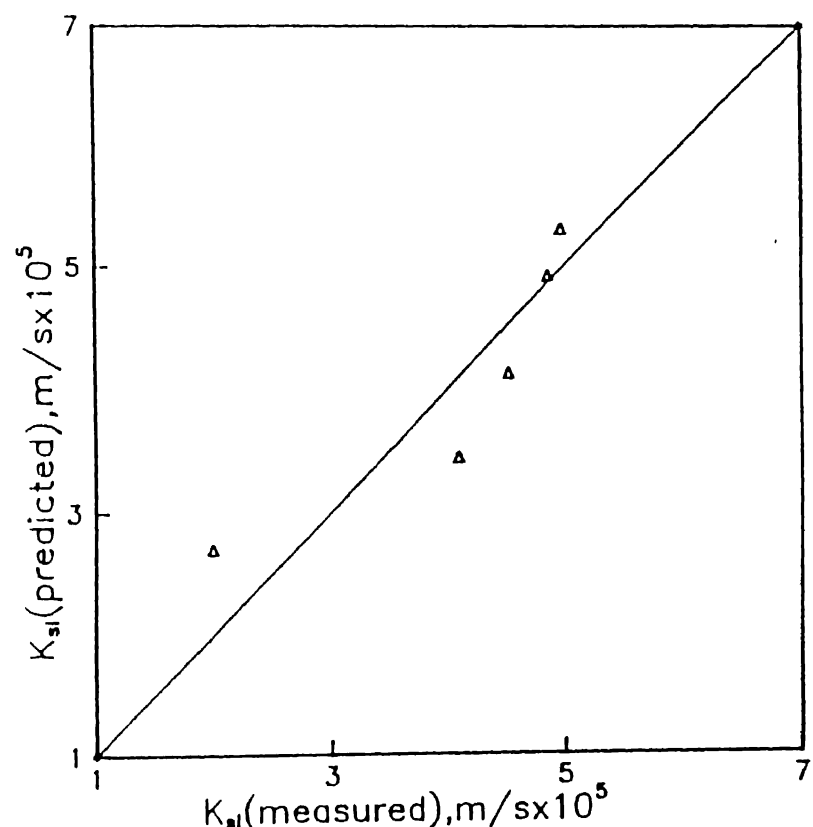


Fig. 3.6 Comparison between measured and predicted values of  $K_{sl}$   
(baffled condition)

amperage given by respective meters. The reason may be due to the variance in design and operating parameters used in our investigation.

For a baffled tank the power consumption was observed to be slightly higher than that of an unbaffled tank. For baffled condition, the plot between measured and correlated values of  $K_{sl}$  is shown in Fig.3.6.

### 3.2 AIR AGITATED TANKS

---

As established in chapter 2, most of the experiments were carried out for 0.002N KCl solution and 0.2wt. % of resin at 20°C to ensure that the leaching process was under external mass transport control regime. The draft tube to tank diameter ratio ( $D_d/D_t$ ) was changed by changing the draft tube diameter keeping the tank diameter constant. The tank height to diameter ratio ( $H_t/D_t$ ) was varied by changing the water level and consequently the length of the draft tube.

#### 3.2.1 Effect of Superficial Gas Velocity on $K_{sl}$

---

The effect of superficial gas velocity ( $U_g$ ) on  $K_{sl}$  for three different  $D_d/D_t$  values, namely, 0.08, 0.18 and 0.3 and for three different  $H_t/D_t$ , viz., 1.5, 2.0 and 2.5 is shown in figs.3.7 to 3.9. For all cases shown in figures, it was observed that  $K_{sl}$

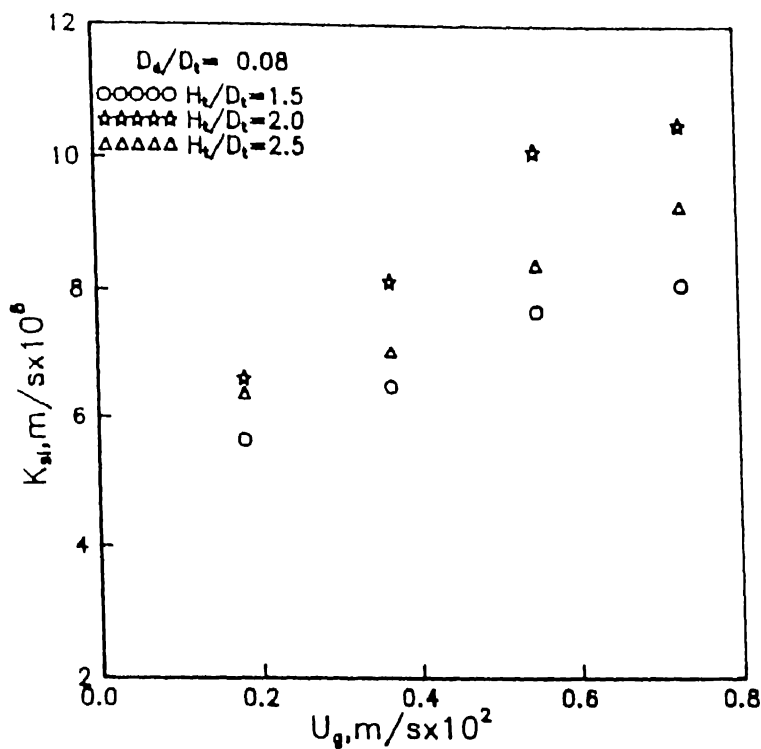


Fig. 3.7 Effect of superficial gas velocity on  $K_{sl}$   
with  $D_d/D_t = 0.08$  in FCC tanks

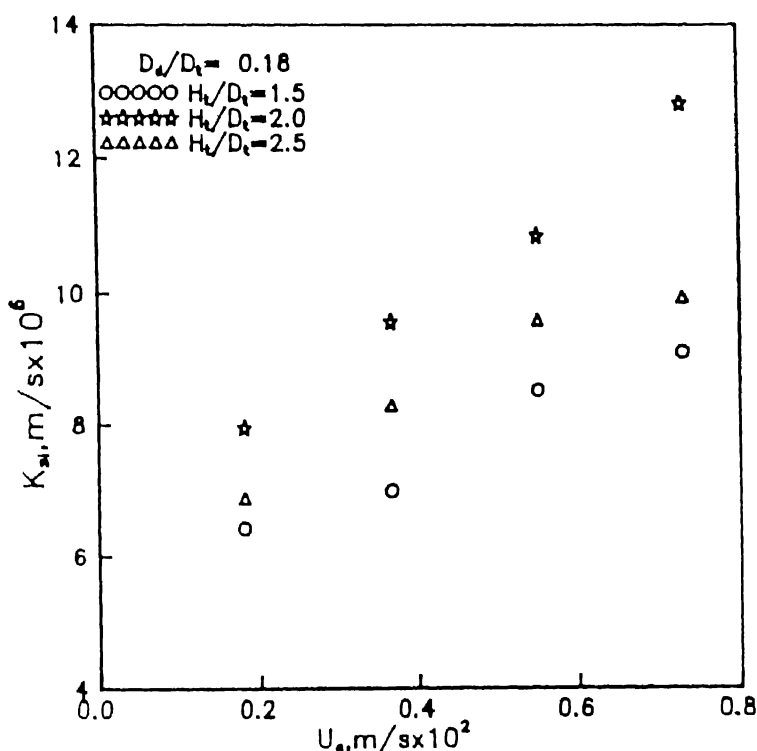


Fig. 3.8 Effect of superficial gas velocity on  $K_{sl}$   
with  $D_d/D_t = 0.18$  in FCC tanks

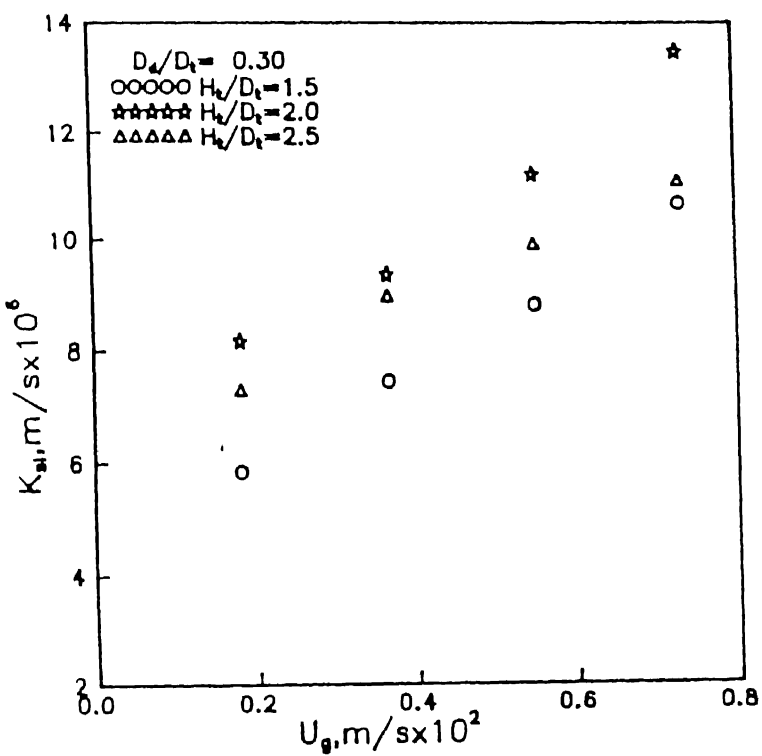


Fig. 3.9 Effect of superficial gas velocity on  $K_{sl}$   
with  $D_d/D_t = 0.30$  in FCC tanks

increased with increasing  $U_g$ . While for  $D_d/D_t$  equal to 0.08 a decrease in the slopes of the curves is evident at higher velocities (Fig.3.7), the slopes remain more or less constant for  $D_d/D_t$  equal to 0.3.

The increase in  $K_{sl}$  with increasing  $U_g$  was attributed to increased turbulence levels as reported by several other investigators (9,10 and 12). Shekhar and Evans (12,13) experimentally measured the liquid velocities and turbulence levels using Laser Doppler velocimeter (for  $D_d/D_t$  equal to 0.13 & 0.26,  $H_t/D_t$  equal to 1.4 & 2.1 and  $U_g$  varied from 0.14 to 0.28 cm/sec) and reported higher values for higher superficial gas velocities. Petrovic et al.(21) observed that an increase in  $U_g$  led to reduction in the circulation and the mixing times, for  $D_d/D_t$  equal to 0.4.

It will, therefore, be more meaningful if the liquid circulation velocities are calculated in the annulus. Calculations of liquid velocity in the annulus are important than the draft tube since it occupies more than 80% of the total tank volume. A model developed by Shekhar et al.(13) has been used to calculate the superficial liquid velocities. Three equations were simultaneously solved to obtain the velocities, which are given below:

$$g \times \phi_d \times H_d = \{ (f_d \times H_d/D_d) + k_{ru} + k_{rl} \} (U_{ld}^2 / 2) \quad -- (3.1)$$

$$U'_{ld} = \{ U_{ld} / (1 - \phi_d) \} \quad -- (3.2)$$

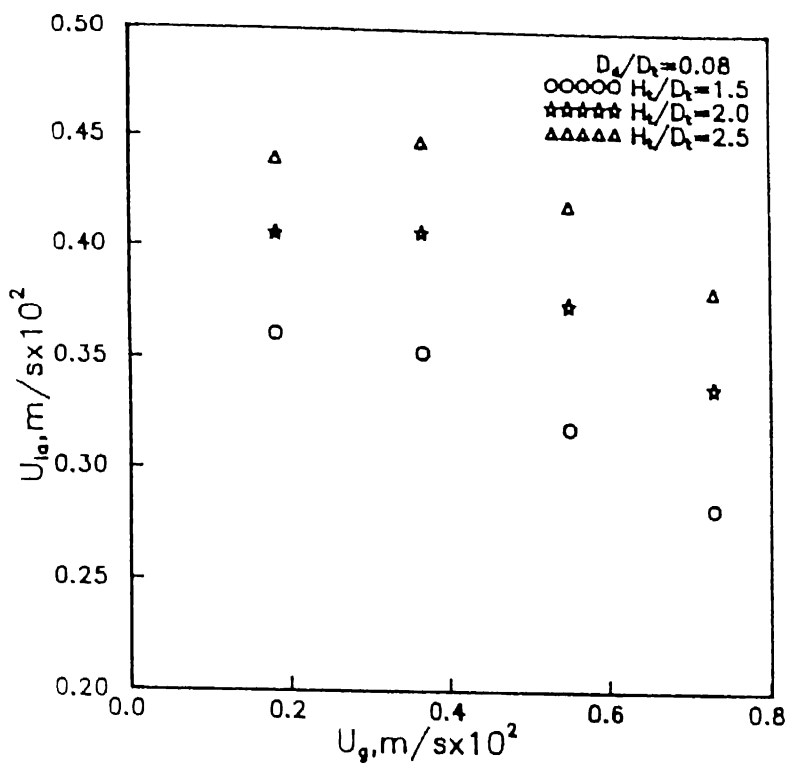


Fig. 3.10 Effect of superficial gas velocity on  $U_{la}$   
with  $D_d/D_t = 0.08$  in FCC tanks

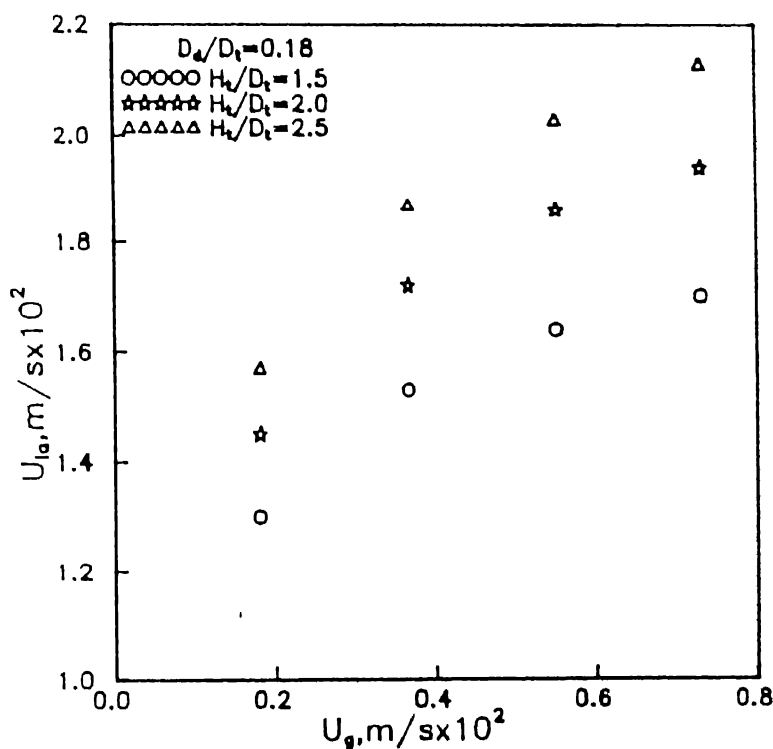


Fig. 3.11 Effect of superficial gas velocity on  $U_{la}$   
with  $D_d/D_t = 0.18$  in FCC tanks

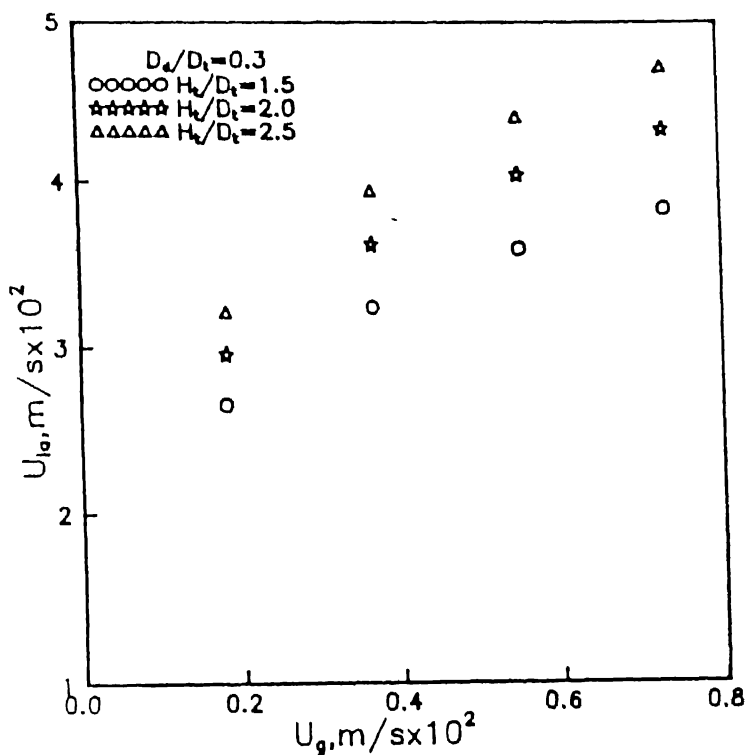


Fig. 3.12 Effect of superficial gas velocity on  $U_{la}$   
with  $D_d/D_t = 0.30$  in FCC tanks

slugs adversely effect the mass transfer as the solid particles are trapped in these slugs, consequently reducing the solid/liquid contact. Furthermore the liquid circulation velocity also decreases because of almost negligible amount of the liquid within the air slugs (9 and 10).

In the case of draft tubes of higher diameters,  $D_d/D_t$  equal to 0.18 and 0.3,  $U_{la}$  increases with increasing  $U_g$  as shown in Fig.3.11 for  $D_d/D_t$  equal to 0.18 and Fig.3.12 for  $D_d/D_t$  equal to 0.3. Increased  $U_{la}$  gives rise to higher mixing rates which, in turn, increases the mass transfer coefficient. Coalescence of air bubbles was not observed in the tanks equipped with draft tubes of larger diameters. The above results were in conformity with the results of previous investigators who observed that for a given  $D_d/D_t$  and  $H_t/D_t$ , both liquid velocity and turbulence levels in the annulus increased with  $U_g$  (12).

### 3.2.2 Effect of Height to Diameter Ratio of Liquid Column on $K_{sl}$

The results for three different draft tubes are shown in Figs.3.13 to 3.15. The figures are for  $D_d/D_t$  ratios of 0.08, 0.18 and 0.3, respectively. From these figures one can see that mass transfer coefficient exhibits a maximum with respect to  $H_t/D_t$  ratio -  $K_{sl}$  increasing for  $H_t/D_t$  values between 1.5 to 2.0 and then decreasing.

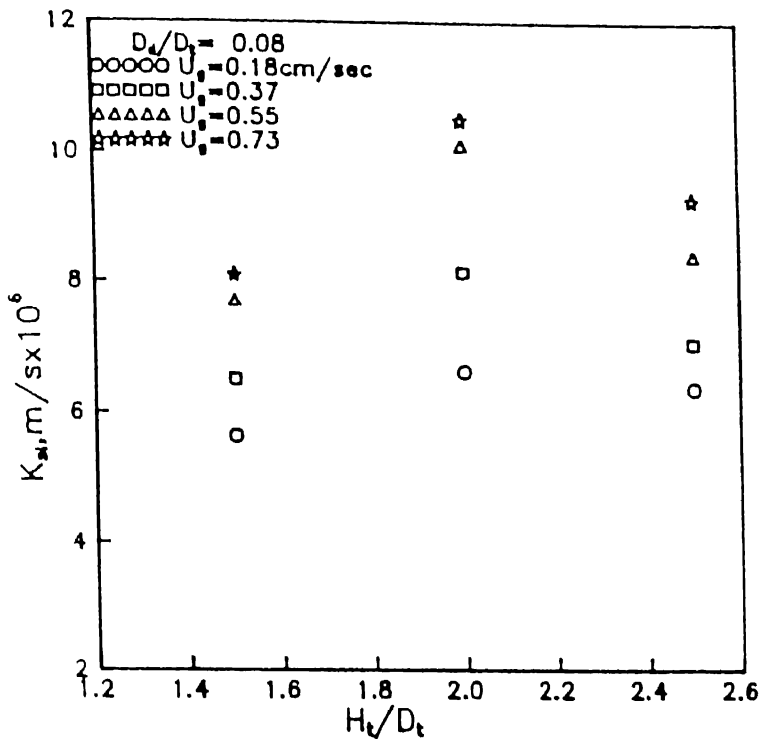


Fig. 3.13 Effect of the liquid column height on  $K_{sl}$   
with  $D_d/D_t = 0.08$  in FCC tanks

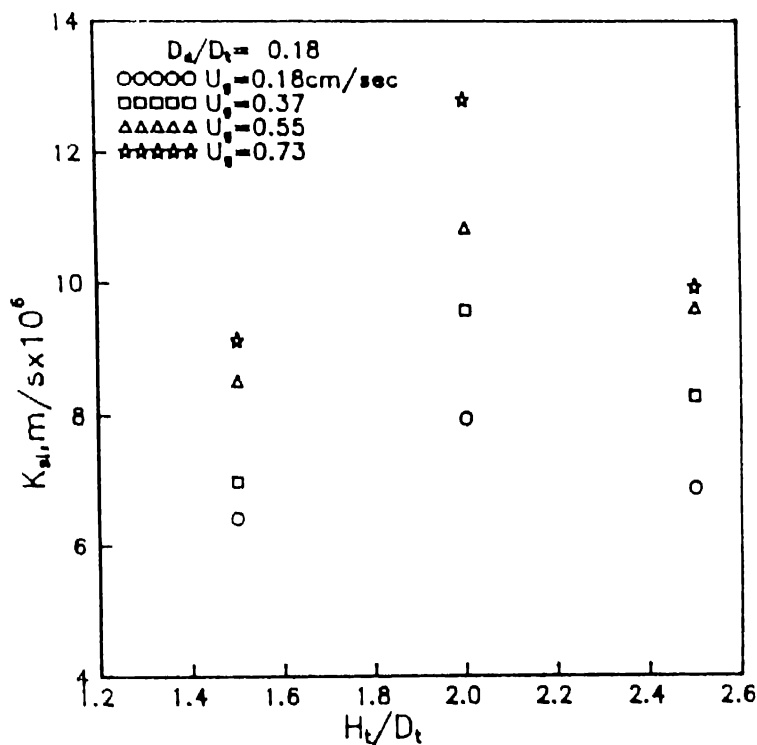


Fig. 3.14 Effect of the liquid column height on  $K_{sl}$   
with  $D_d/D_t = 0.18$  in FCC tanks

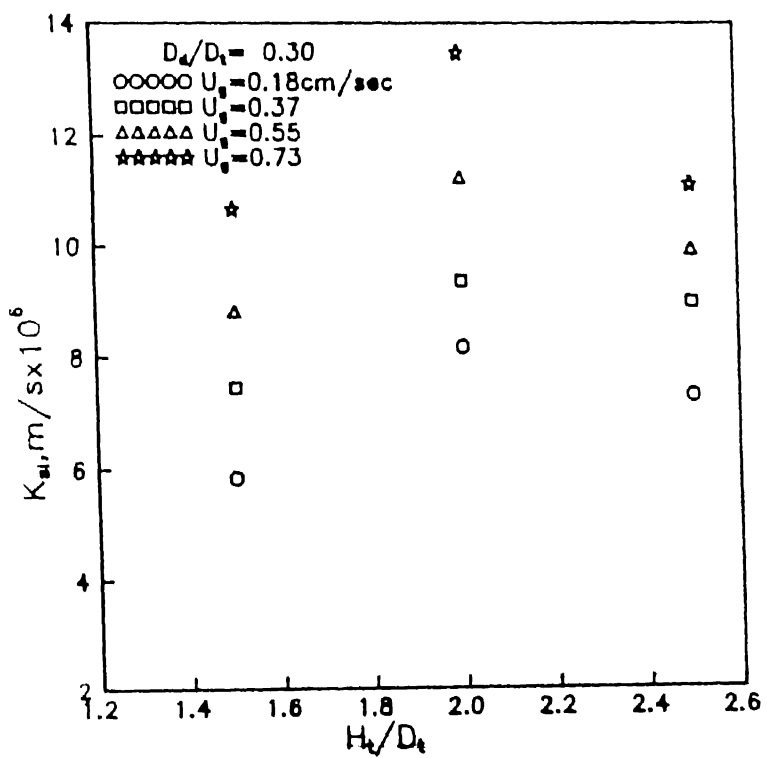


Fig. 3.15 Effect of the liquid column height on  $K_{sl}$   
with  $D_d/D_t = 0.30$  in FCC tanks

Again liquid velocities in both the draft tube and the annulus were calculated for different heights of liquid column. Figs.3.16 to 3.18 show the effect of  $H_t/D_t$  on  $U_{ld}$ . The velocities in the annulus were observed to increase with increasing  $H_t/D_t$  value. A theoretical equation given by Chisti et al.(23) predicted that increase in liquid circulation is proportional to the square root of the dispersion height. The equation is given as,

$$U_{ld} = \frac{2.0 \times g \times (\phi_d - \phi_a) \times H_d}{K_t \times (1/(1-\phi_d^2)) + K_b \times ((A_d/A_a^2) \times (1/(1-\phi_a^2)))} \quad \text{-- (3.4)}$$

where  $K_t$  and  $K_b$  are frictional loss coefficients at the top and bottom connecting sections. He supported his theoretical predictions by experimental measurements. His predicted as well as experimental results do not show the optimum in  $K_{sl}$  with  $H_t/D_t$ .

It is, therefore, speculates that there in one other factor other than the liquid velocity - which is affecting the  $K_{sl}$  values at higher  $H_t/D_t$ . Shekhar et al.(12,13) have reported the presence of a stagnant zone which extends from above the cone to midsection of annulus in tanks of  $H_t/D_t$  equal to 2.1. The presence of this zone is undesirable since it consumes energy and is likely to provide little in terms of mass transfer. On the other hand, they observed that the stagnant zone was eliminated in shallower

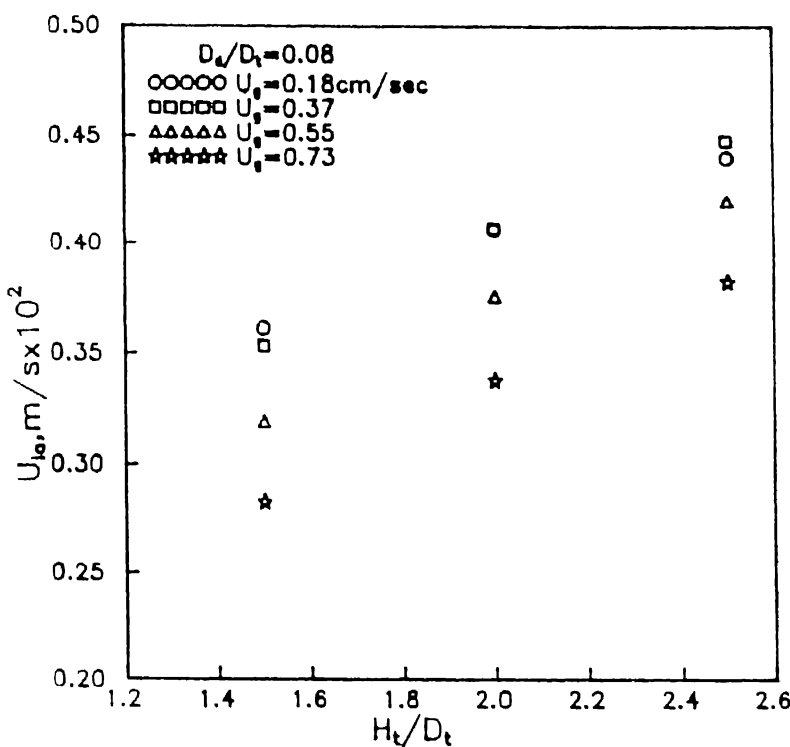


Fig. 3.16 Effect of height of the liquid column on  $U_{\text{liquid}}$   
with  $D_d/D_t = 0.08$  in FCC tanks

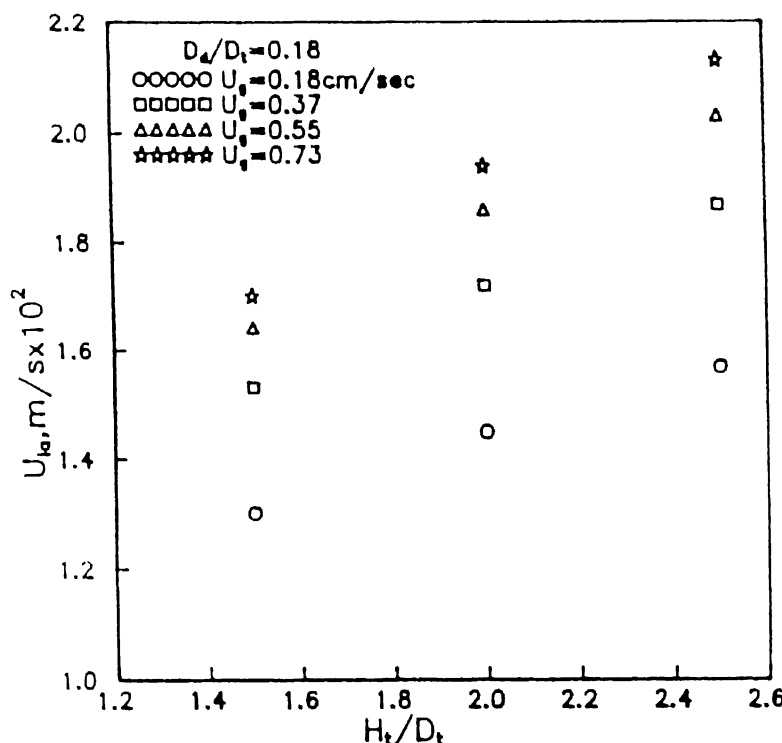


Fig. 3.17 Effect of height of the liquid column on  $U_{\text{liquid}}$   
with  $D_d/D_t = 0.18$  in FCC tanks

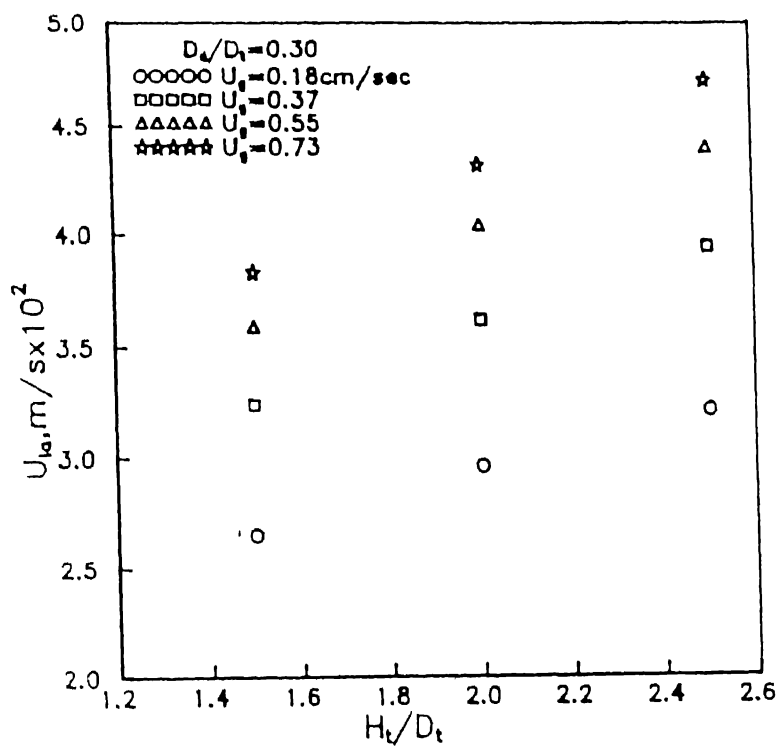


Fig. 3.18 Effect of height of the liquid column on  $U_{la}$   
with  $D_d/D_t = 0.30$  in FCC tanks

tanks ( $H_t/D_t$  equal to 1.3), although the maximum velocities are lower than those of deeper tanks. Also, turbulence levels were more uniformly distributed in smaller liquid columns. The fact was also confirmed by the measurements of  $K_{gl}$ , by Roy et al.(27), who found that  $K_{gl}$  at the bottom of the tank was about 60% of the  $K_{gl}$  near the top of the tank at  $H_t/D_t$  equal to 2.0.

Occurrence of the maximum in  $K_{sl}$  verses  $H_t/D_t$  plots may be explained incorporating the presence of the stagnant zone. The turbulence levels in the annulus probably increased with  $H_t/D_t$ , up to a ratio of 2.0. So  $K_{sl}$  increased with increasing  $H_t/D_t$ . However for  $H_t/D_t$  greater than 2.0 the control was shifted to the stagnant zone which is building up in the annulus from mid section to the bottom of cone, as the height of liquid column increases. This results in reduction in  $K_{sl}$  above a value of  $H_t/D_t$  equal to 2.0.

### 3.2.3 Effect of the Draft Tube to Tank Diameter Ratio on $K_{sl}$

As already mentioned experiments were carried out for three different  $H_t/D_t$ , namely, 1.5, 2.0 and 2.5, with  $D_d/D_t$  ratio varying between 0.08 and 0.3. Variation of  $K_{sl}$  with  $D_d/D_t$  for various  $U_g$  values and a constant  $H_t/D_t$  value is shown in figs.3.19, 3.20 and 3.21. An increasing trend for  $K_{sl}$  was obtained with increasing  $D_d/D_t$ . This increase in  $K_{sl}$  was attributed to the increased liquid circulation and enhanced degree of turbulence in

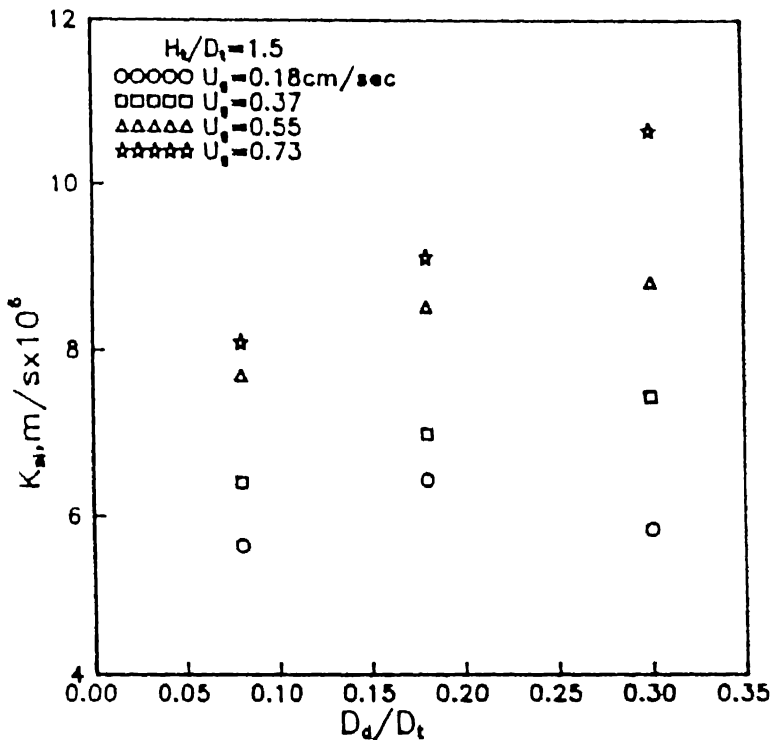


Fig. 3.19 Effect of the draft tube diameter on  $K_{sl}$   
with  $H_t/D_t = 1.5$  in FCC tanks

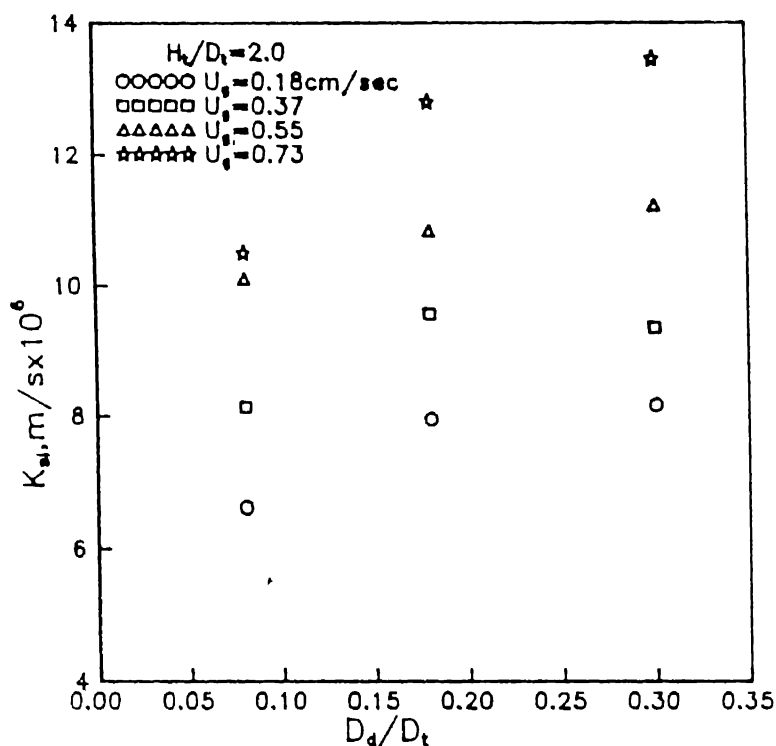


Fig. 3.20 Effect of the draft tube diameter on  $K_{sl}$   
with  $H_t/D_t = 2.0$  in FCC tanks

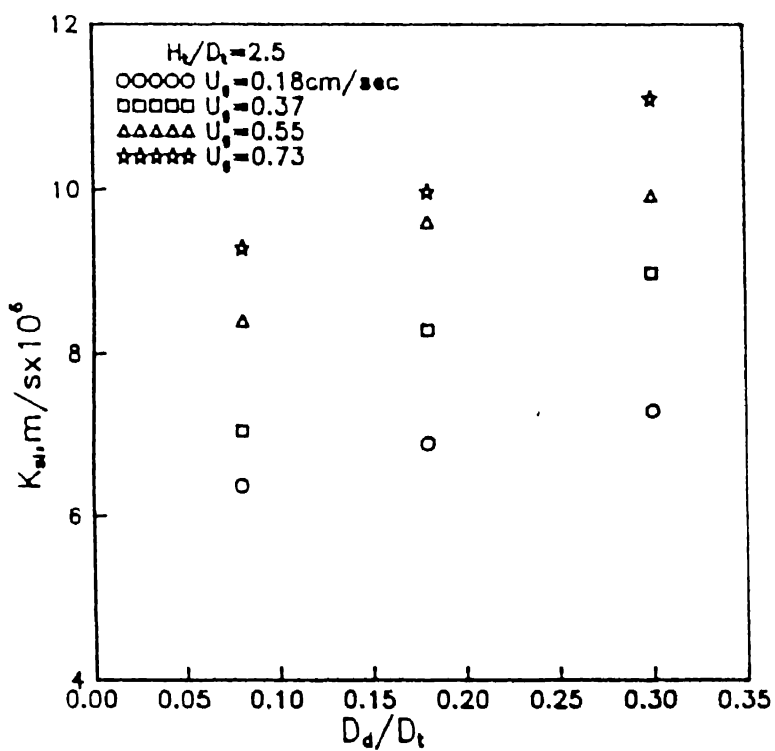


Fig. 3.21 Effect of the draft tube diameter on  $K_{sl}$   
with  $H_t/D_t = 2.5$  in FCC tanks

the annulus with increasing  $D_d/D_t$  (12 & 24). Measurements of the liquid velocities and turbulence levels by Shekhar et al.(12) using LDV, have shown higher values for the tanks equipped with bigger draft tubes ( $D_d/D_t = 0.26$ ) than narrower one ( $D_d/D_t = 0.13$ ). Weiland(24) found that the liquid flow rate for a given  $U_g$  goes through a maximum at  $D_d/D_t$  equal to 0.6 and then decreases with the further increase in draft tube diameter.

To establish that this indeed is the case, liquid velocities in the annulus  $U_{la}$  were computed for different draft tube diameters using the model proposed by shekhar et al.(12). Computed  $U_{la}$  values for various  $D_d/D_t$ ,  $H_t/D_t$  values and for different superficial gas velocities are plotted in figs.3.22, 3.23 and 3.24. It is to be noted that  $U_{la}$  increases quite substantially with increasing  $D_d/D_t$ . Hence, increase in  $U_{la}$  leads to enhanced liquid circulation and turbulence levels. Therefore higher  $K_{sl}$  values. These observations were in conformity with those of, Shekhar et al. who reported that for a given  $H_t/D_t$  and  $U_g$ , turbulence level within the annulus increased with  $D_d/D_t$  (12) and Weiland(22) who has reported increase in liquid circulation velocities with  $D_d/D_t$  up to a value of 0.6.

### 3.2.4 Correlation Between $K_{sl}$ and Power Input

The energy input to the system comes primarily from the

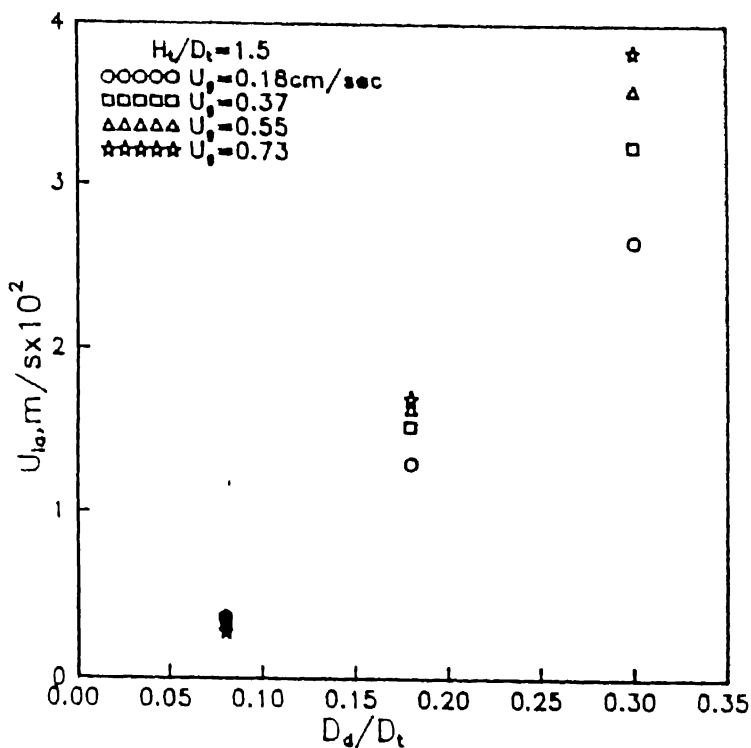


Fig. 3.22 Effect of the draft tube diameter on  $U_{la}$   
with  $H_t/D_t = 1.5$  in FCC tanks

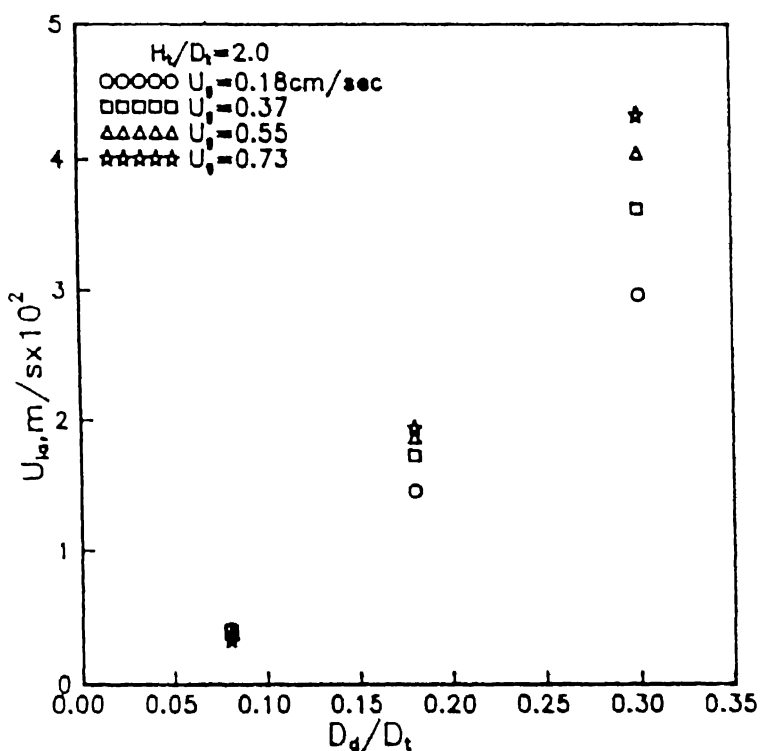


Fig. 3.23 Effect of the draft tube diameter on  $U_{la}$   
with  $H_t/D_t = 2.0$  in FCC tanks

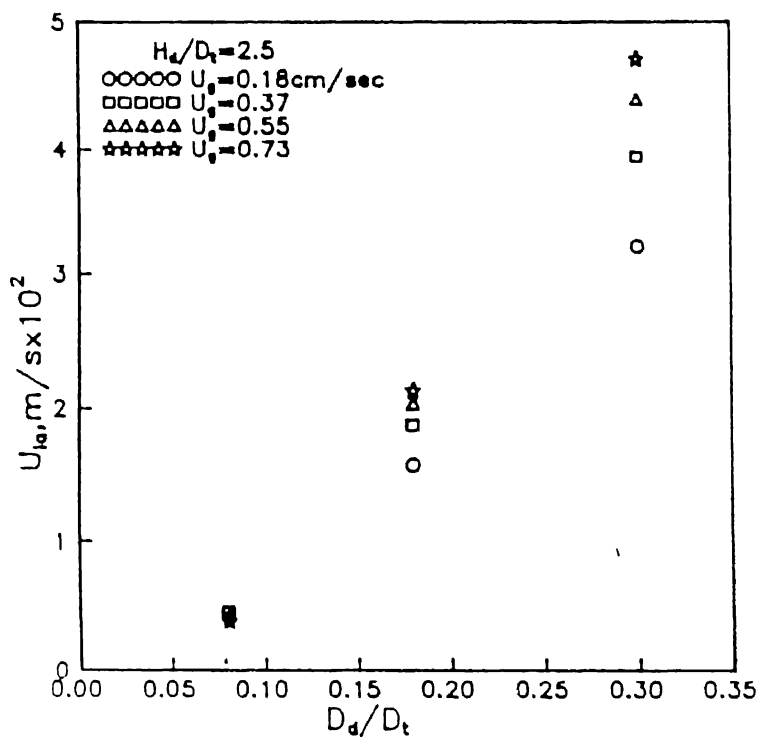


Fig. 3.24 Effect of the draft tube diameter on  $U_{1a}$   
with  $H_t/D_t = 2.5$  in FCC tanks

isothermal expansion of air as it moves up in the draft tube -the kinetic energy component of the jet from the nozzle is usually small and can be disregarded (23). Energy is dissipated in the form of, wall friction in the draft tube and the annulus, friction and drag as fluid reverses its direction of flow at the top and the bottom zones of the tank and liquid circulation in the wakes behind the air bubbles. The energy input can be calculated using the equation proposed by Krishna Murthy et al.(25) for gas agitated liquid baths. The equation for energy input per unit volume is as following:

$$\varepsilon = \frac{4.0 \times Q \times T_l \times P_{atm}}{298.2 \times \pi \times D^2 \times H} \times \ln \left\{ 1.0 + \frac{\rho \times g \times H}{P_{atm}} \right\} \quad \text{-- (3.5)}$$

An attempt has been made to establish a correlation between the  $K_{sl}$  and the power input per unit volume of the liquid in the tank. The best correlation that could be obtained with single variable is

$$K_{sl} = 0.0104 (\varepsilon)^{0.296}$$

A plot of this correlation is presented in fig.3.25. As it may be noted, this correlation is not very satisfactory. To obtain a more meaningful correlation,  $H_t/D_t$  and  $D_d/D_t$  were also included as variables and a correlation with the three variables was obtained.

$$K_{sl} = 2.465 (\varepsilon)^{0.310} (D_d/D_t)^{0.112} (H_t/D_t)^{0.359}$$

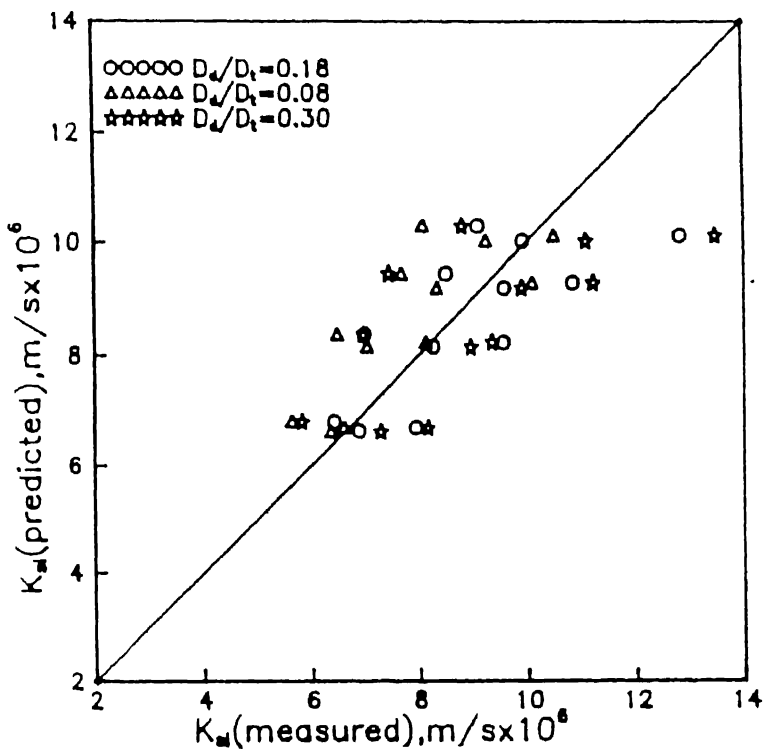


Fig. 3.25 Comparison between measured and predicted values of  $K_{s1}$

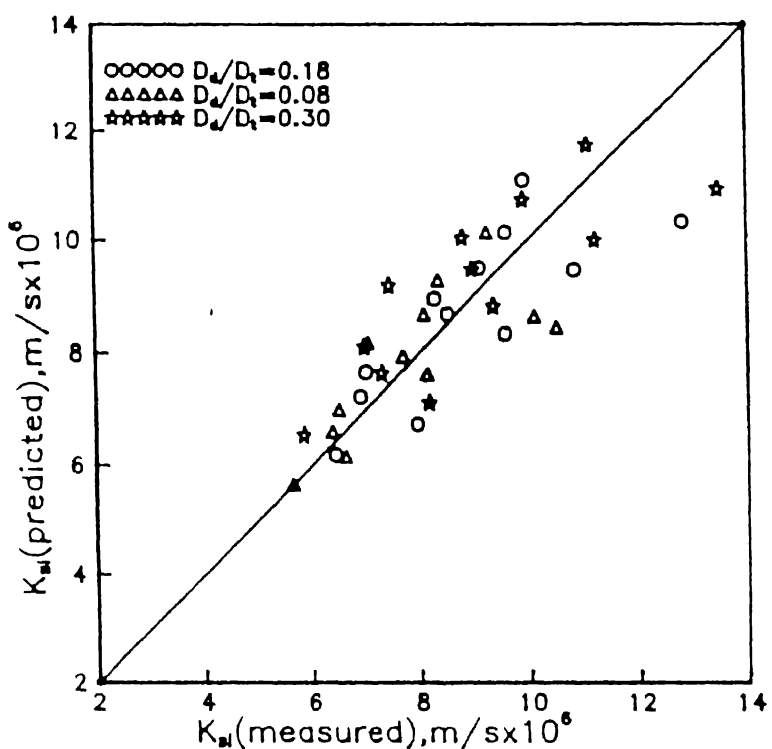


Fig. 3.26 Comparison between measured and predicted values of  $K_{s1}$

A plot of measured and correlated values of  $K_{sl}$  is shown in fig.3.26. From this plot it can be concluded that the proposed three variable correlation is quite satisfactory.

### 3.2.5 Stub Column type Tanks (SCT)

---

The design of the original pachuca tank was somewhat modified to study the effect of Stub Column type (SC) configuration on  $K_{sl}$ . Generally, a SC tank is operated with draft tube of heights almost half of those used in a Full Center Column (FCC) tank. For our investigation, experiments were carried out using a draft tube of  $D_d/D_t$  equal to 0.18 and  $H_d/D_t$  equal to 0.723. The effect of liquid column height on  $K_{sl}$  was also studied by varying the liquid levels in this tank but using the same draft tube.

Velocity measurements by Shekhar et al.(12) shown that the top section of the SC tank was more vigorously agitated as compared to a FCC tank. In fact, the hydrodynamics of the SC tank is expected to be similar to that of a Free Air Lift (FAL) tank (discussed below) above the top of the draft tube and also to that in a FCC tank in the region extending below the top of the draft tube.

---

Effect of Superficial Gas Velocity on  $K_{sl}$  : The effect of  $U_g$  on  $K_{sl}$  in a SC tank is similar to that in a FCC tank i.e.  $K_{sl}$  increases with increasing  $U_g$ . This pattern is observed for all heights of

liquid columns (see fig.3.27) which were examined in this case. An increase in the degree of turbulence due to increased  $U_g$  may be a plausible reason for an increase in  $K_{sl}$ .

Effect of the Liquid Column Height on  $K_{sl}$  : Fig.3.28 shows the

effect of liquid column height on  $K_{sl}$  in a SC tank. Unlike a FCC tank where  $K_{sl}$  exhibits a maxima with respect to  $H_t/D_t$ , in a SC tank  $K_{sl}$  increases monotonically. The factor which perhaps contributes for increasing  $K_{sl}$  at high  $H_t/D_t$  is the following. As mentioned earlier, in case of a FCC tank the stagnant zone seems to be dominant at higher  $H_t/D_t$  values. In the case of SC tank, however, the stagnant zone is not dominant, as is evident from measurements of gas-liquid mass transfer coefficient by Roy et al.(27) and turbulent kinetic energy measurement by Shekhar and Evans(12).

### 3.2.6 Free Air-lift Tanks (FAL)

As mentioned earlier in chapter 2, higher flow rates have been used in Free Air-lifts (FAL) because of the difficulty in keeping the particles in suspension. Using two side tubes (as shown in fig 2.14) and keeping a constant gas flow rate(5 lpm i.e.0.46cm/sec of  $U_g$ ) within these side tubes, the gas flow rate through the central tube has been varied from 2 to 8 lpm ( $U_g$  from 0.18 to 0.73cm/sec). Experiments have been carried out for different heights of liquid columns ranging from 1.5 to 2.5  $H_t/D_t$ .

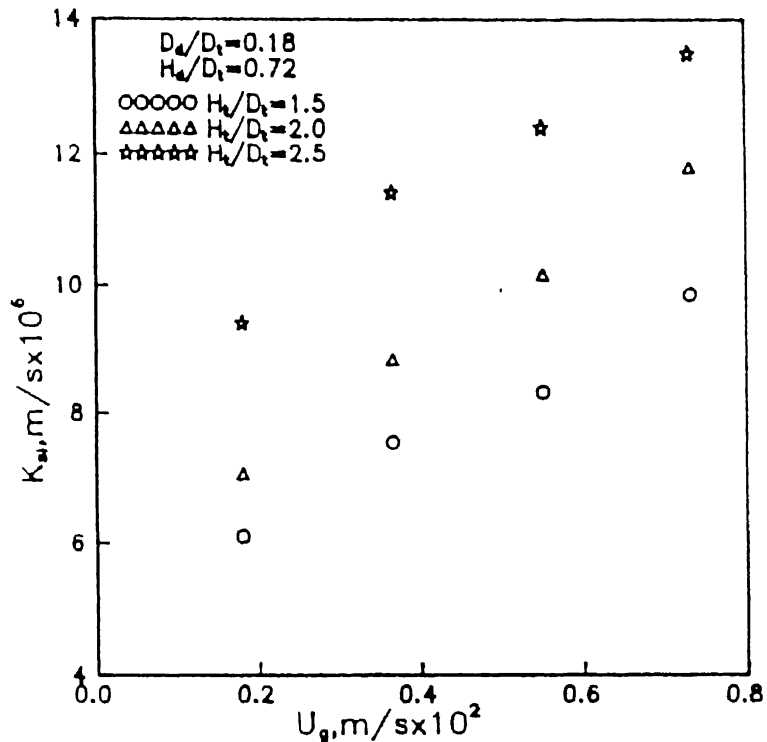


Fig. 3.27 Effect of superficial gas velocity on  $K_{sl}$  in SCT tanks

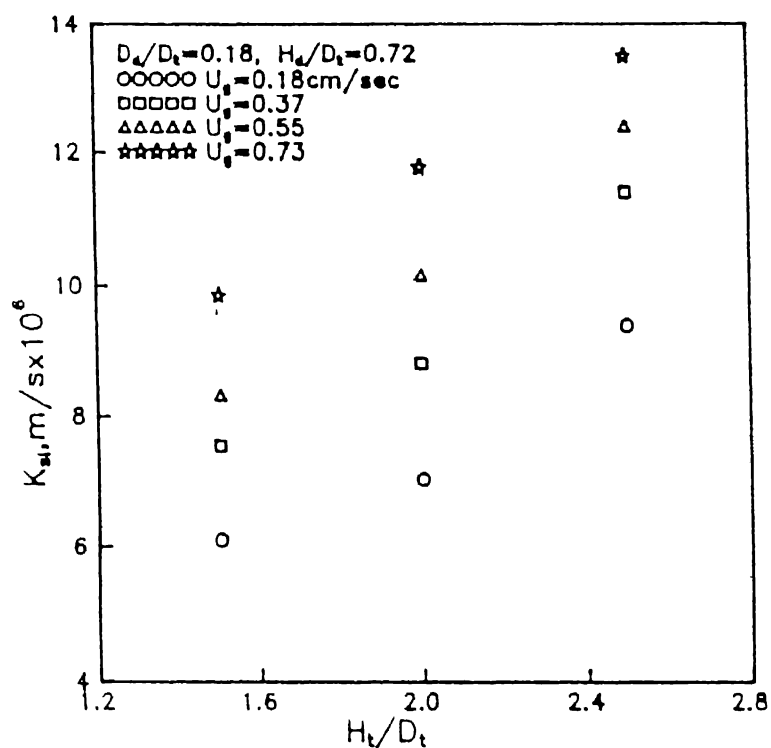


Fig. 3.28 Effect of tank height on  $K_{sl}$  in SCT tanks

Effect of Superficial Gas Velocity on  $K_{sl}$  : Effect of  $U_g$  on  $K_{sl}$  in a

FAL tank is shown in figure 3.29, where the total superficial gas velocity was varied from 0.64 to 1.19 cm/sec.  $K_{sl}$  values were observed to be increased with increasing  $U_g$  irrespective of the height of liquid column. This increase in  $K_{sl}$  may be due to the increased turbulence in liquid phase observed at higher gas flow rates. Aforestated trend has also been mentioned by some other investigators (3, 8, 9 and 10). However, the flattening of the  $K_{sl}$  versus  $U_g$  curve at higher  $U_g$  values as reported by these investigators, has not been noticed in the present investigation.

Effect of Height of the Liquid Column on  $K_{sl}$  : Fig.3.30 shows the

effect of the liquid column height on  $K_{sl}$ , in which the latter increases monotonically for  $H_t/D_t$  varying between 1.5 and 2.5. The increase in  $K_{sl}$  may be due to higher turbulence levels observed in deeper tanks, because of the higher energy that is supplied by air at higher  $H_t/D_t$ .

However, the  $K_{sl}$  versus  $H_t/D_t$  curve for the FAL tank was not as steep as it is for the SC tank, after a  $H_t/D_t$  value of 2.0. The possible explanation may be given as following. Shekhar et al.(12) have reported that for both SC and FAL tanks, the stagnant zone is less prominent compared to a FCC tank for a  $H_t/D_t$  value of 2.1.

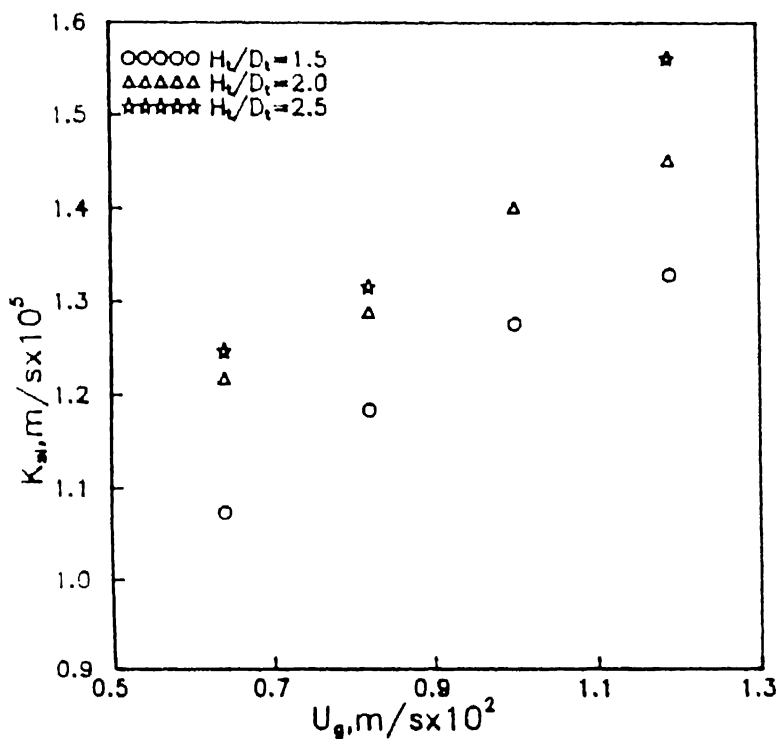


Fig. 3.29 Effect of Superficial gas velocity on  $K_{sl}$  in FAL tanks

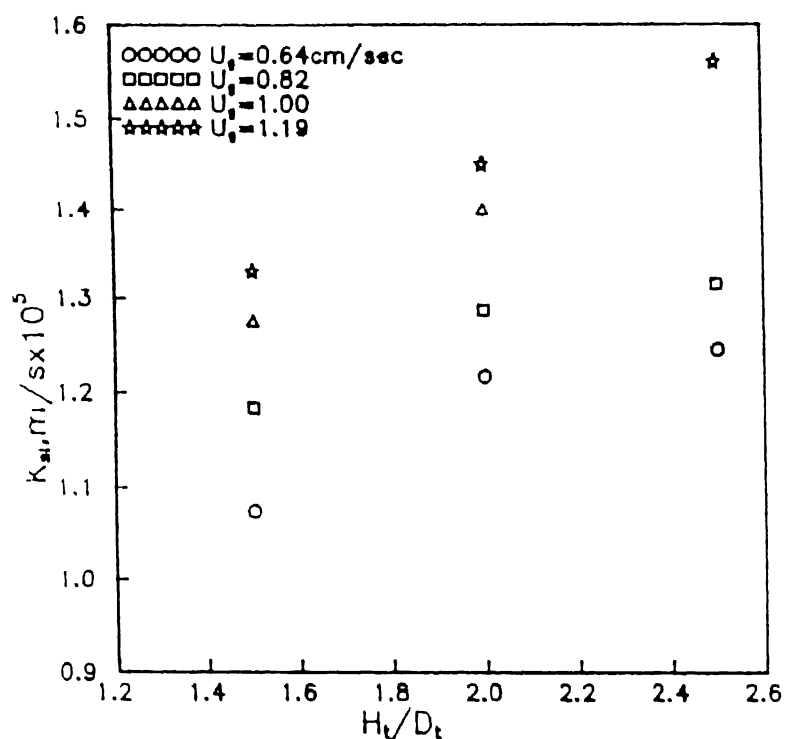


Fig. 3.30 Effect of tank Height on  $K_{sl}$  in FAL tanks

Effect of height of liquid column was observed by Jadhav et al.(9), in which  $K_{sl}$  was noticed to be independent of height of column. However they have carried out their experiments at much higher values of  $H_t/D_t$  equal to 4-13. Hence it is not feasible to compare the results of FAL tanks (operated at  $H_t/D_t$  between 1.5 to 2.5) with this investigation.

### 3.2.7 Comparison Between FCC,SC and FAL Configurations

---

Comparison of all the three configurations (FCC, FAL and SC) can now be made in terms of  $K_{sl}$  plotted against  $U_g$ , for a fixed liquid column height and for the same draft tube diameter. Figs.3.31 to 3.33 compare the behavior of the three types of pachucas for different  $H_t/D_t$  values 1.5, 2.0 and 2.5, respectively. Because of the difference in design and operating parameters in the FAL tank, it is not feasible to compare the values of  $K_{sl}$  with FCC and SC configurations.

For  $H_t/D_t$  equal to 1.5,  $K_{sl}$  values were almost the same for both FCC and SC configurations. But higher for the FAL configuration (fig.3.31). For a ratio of Height to diameter 2.0,  $K_{sl}$  values were observed to be almost independent of the tank design (fig.3.32). From Fig.3.33, it can be seen that  $K_{sl}$  values are equal for FAL and SC tanks where as lower values were observed for FCC, at  $H_t/D_t$  of 2.5.

At smaller  $H_t/D_t$  values  $K_{sl}$  for SC and FCC was observed to be same and the difference increases with increase in  $H_t/D_t$ , with greater values for SC, as expected due to the absence of stagnant zone (fig.3.33).

### 3.2.8 Comparison Between Air and Mechanically Agitated Tanks

---

Comparison of air and mechanically agitated tanks can be done in terms of energy input per unit volume of the liquid in the tank. In mechanically agitated tanks power consumption was calculated directly from the readings given by ammeter and voltmeter. The power input was observed to be varied from 5040 to  $14690 \text{ Kg/m.sec}^3$  when stirrer speed increased from 600 to 1650 rpm. In case of air agitated tanks the energy input per unit volume was calculated from the isothermal expansion of air bubbles through the liquid column in the tank. The calculated power input was varied from 20 to  $85 \text{ Kg/m.sec}^3$  with superficial gas velocity ranging from 0.18 to 0.73 cm/sec.

A plot between the values of  $K_{sl}$  and power input is shown in Fig.3.34, to compare the performance of both air and mechanically agitated tanks. From the above figure it can be noted down that air agitated tanks were effective in solid-liquid dissolution process compared to mechanical agitation, for the same power input. In air agitated tanks, SC and FAL configurations were observed to be

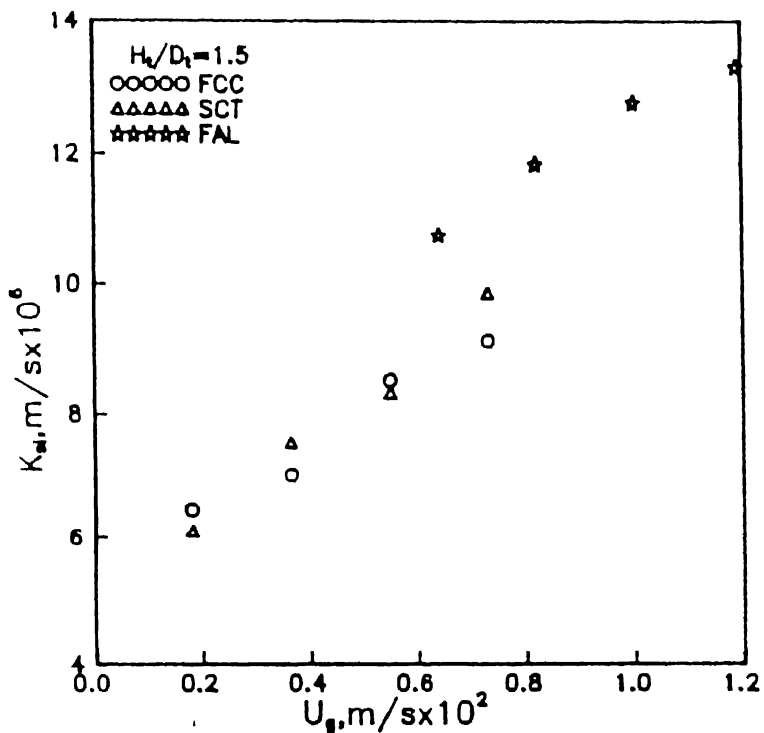


Fig. 3.31 Effect of tank design on  $K_{sl}$  at  $H_t/D_t = 1.5$

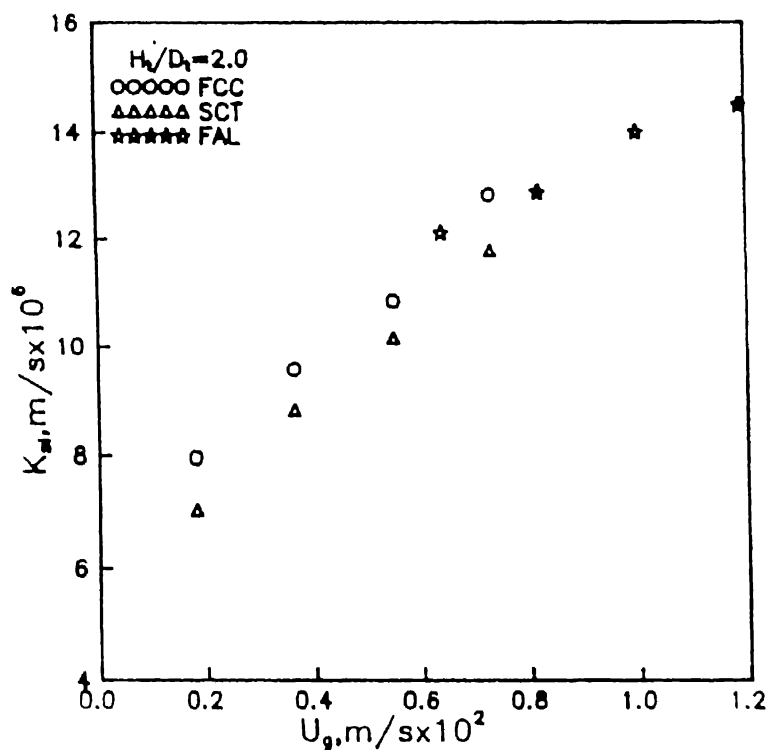


Fig. 3.32 Effect of tank design on  $K_{sl}$  at  $H_t/D_t = 2.0$

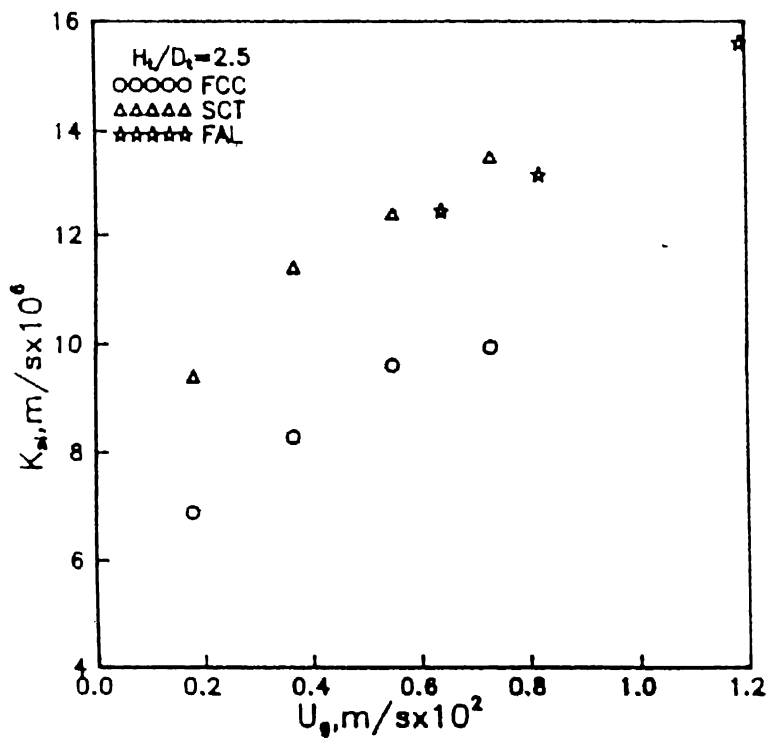


Fig. 3.33 Effect of tank design on  $K_{sl}$  at  $H_t/D_t = 2.5$

superior to FCC tanks for the same power input per unit volume of the liquid.

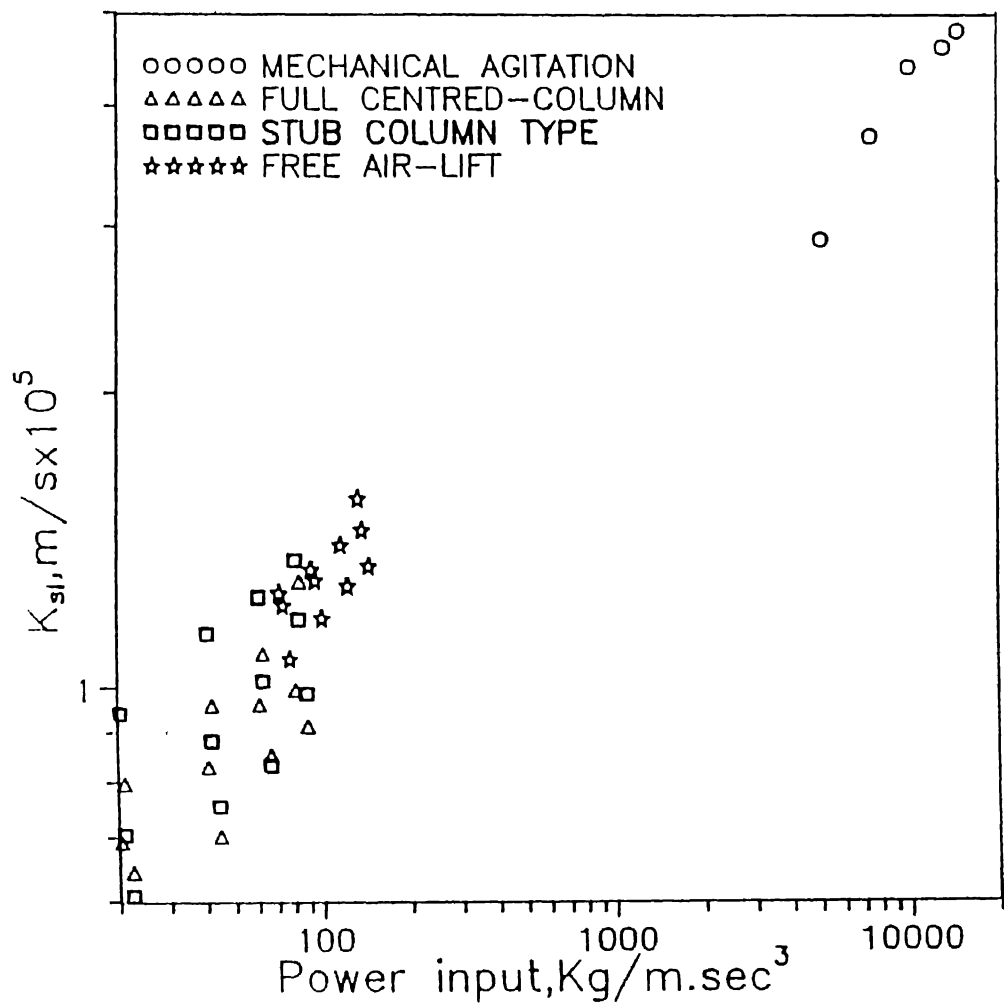


Fig. 3.34 Comparison of air and mechanically agitated tanks

## CHAPTER IV

### CONCLUSIONS

This investigation has examined the effect of design and operating parameters of air agitated pachuca tanks such as superficial gas velocity, tank height to diameter and draft tube to tank diameter ratios on solid-liquid mass transfer coefficient ( $K_{sl}$ ). In addition, experiments were also conducted in mechanically-agitated tanks to make a preliminary comparison of power consumption with air-agitated pachuca tanks.

Some of the important conclusions emerging from this work are:

(1) Irrespective of the tank design  $K_{sl}$  increased with  $U_g$ . However, for Full Center Column tanks equipped with smaller draft tubes  $K_{sl}$  tends to become independent of  $U_g$  at superficial gas velocities greater than 0.6 cm/sec.

(2) For a given  $D_d/D_t$  value in Full Center Column,  $K_{sl}$  increases when  $H_t/D_t$  increases from 1.5 to 2.0. However, a further increase in  $H_t/D_t$  to 2.5 leads to a reduction in  $K_{sl}$ .

(3) In a Full Center Column for a fixed  $H_t/D_t$ ,  $K_{sl}$  increased monotonically with draft tube diameter with in the range of  $D_d/D_t$  equal to 0.08 to 0.3.

(4) For stub column tanks, unlike Full Center Column tanks,  $K_{sl}$

increased continuously with  $H_t/D_t$  throughout the range (1.5 to 2.5) that was investigated.

(5) At  $H_t/D_t$  ratios of 1.5 and 2.0,  $K_{sl}$  was independent of configuration, that is similar values were observed in both Stub Column and Full Center Column tanks. On the other hand, higher values of  $K_{sl}$  were observed for stub column tanks at an  $H_t/D_t$  ratio of 2.5. It was not possible to compare the FAL tanks with FCC and SC tanks, FAL tanks were operated at different design and operating parameters because of problems encountered in suspending the resins.

(6) Air agitated tanks seem to be efficient in terms of power input per unit volume of the system, compared to mechanically agitated tanks.

However, more experiments in tanks of different diameters have to be conducted before the conclusions can be deemed reliable.

## APPENDIX

### SAMPLE CALCULATION

A plot of  $K^+$  concentration with time will yield  $K_{sl}$ :

$$- (dY_b/dt) * C_0 * V = K_{sl} * A * (Y_b - Y_t) * C \quad \text{--- (1)}$$

To ensure that  $K_{sl}$  corresponds to the condition where external mass transport is the rate controlling step, equation 1 is evaluated at  $t=0$ :

$$K_{sl} = - (V/A) * (dY_b/dt)_{t=0} \quad \text{--- (2)}$$

Correlations can be obtained for different concentrations of solutions and a general correlation equation is given as:

$$\sigma = M * Y_b + \text{constant}$$

Therefore  $K_{sl}$  was evaluated from the following equation:

$$K_{sl} = - (V/A) * (1/M) * (d\sigma/dt)_{t=0} \quad \text{--- (3)}$$

For a run code of 080203 (0.002N KCl solution with 0.2 wt. % of resin in air agitated tank)

$$V = \text{volume of the solution} = 3300 \text{ cm}^3$$

$$A = \text{total surface area} = 1240 \text{ cm}^2$$

$$(d\sigma/dt)_{t=0} = \text{initial slope of the conductivity versus time}$$

data curve = 0.01395 (Data from chart recorder was fitted with a polynomial in Grapher package from which initial slope is calculated).

The correlation between solution conductivity and  $Y_b$  for 0.002N KCl solution is

$$\sigma = -0.548 Y_b + 0.842$$

i.e.  $M = -0.548$

Therefore the mass transfer coefficient was obtained from equation (3) is equal to  $8.66 \times 10^6 \text{ m/s}$ .

Whole data was presented in tables in preceding pages.

DATA IN TABULAR FORM

sl. No.	Run code	$U_g$ (cm/s)	$D_d / D_t$	$H_t / D_t$	$k_{sl}$ m/s $\times 10^6$
------------	-------------	--------------	-------------	-------------	----------------------------

AIR AGITATED TANKS

Full Center Column:

1	070101	0.18	0.18	1.5	6.6
2	060202				6.06
3	100101				6.24
4	020102				6.84
5	190202				6.54
6	190201				6.29
7	170202	0.37	0.18	1.5	7.41
8	170201				7.35
9	060204				6.56
10	040102				7.06
11	050101				6.66
12	120202	0.55	0.18	1.5	7.82
13	120204				8.29
14	050202				8.59
15	050201				8.29
16	110101				9.66
17	130101	0.73	0.18	0.5	11.16
18	130102				9.10
19	080203				8.66
20	030204				9.66
21	080204				9.27
22	080201				8.89
23	140104	0.18	0.18	2.0	8.10
24	180101				8.47
25	190203				7.47
26	190204				7.77
27	150102	0.37	0.18	2.0	8.55
28	140102				10.41
29	170204				10.07
30	170203				9.47

31	050203	0.55	0.18	2.0	10.09
32	140102				12.60
33	180102				10.88
34	140204				10.22
35	140202				10.41
36	020204	0.73	0.18	2.0	12.97
37	140101				12.82
38	150101				13.40
39	120201	0.73	0.18	2.0	12.03
40	120205				12.91
41	190205	0.18	0.18	2.5	6.99
42	180103				6.78
43	190102	0.37	0.18	2.5	9.10
44	220103				8.42
45	180104				7.82
46	170205				8.79
47	170206				8.10
48	190103	0.55	0.18	2.5	10.90
49	050204				9.29
50	180105				9.28
51	140201				9.38
52	140203				8.72
53	190101	0.73	0.18	2.5	9.16
54	230202				10.40
55	020202				10.35
56	180202				9.79
57	240101	0.18	0.08	2.0	6.61
58	240103	0.37			6.49
59	240105	0.55			7.69
60	240102	0.73			8.09
61	250101	0.18	0.08	2.0	6.61
62	250102	0.37			7.29
63	250103	0.77			8.48
64	250104	0.55			10.20
65	200202	0.73			10.50
66	020206	0.73	0.08	2.5	9.28
67	070102	0.73			10.32
68	280104	0.55			8.60
69	280103	0.55			8.17

70	280105	0.37			7.04
71	280101	0.18			7.36
72	200101	0.18	0.30	1.5	8.83
73	200103	0.37			6.97
74	200102	0.37			7.92
74	200104	0.55			8.48
74	200105	0.55			9.13
75	200101	0.73			10.66
76	210102	0.18	0.30	2.5	8.17
77	210104	0.37			9.36
78	220101	0.55			10.87
79	220102	0.55			11.34
80	210203	0.73			13.47
81	290104	0.18	0.30	2.5	7.29
82	290102	0.37			8.97
83	290103	0.55			9.91
84	290101	0.75			12.51

Stub column:

85	310101	0.18	0.18	1.5	6.09
86	310102	0.37			7.54
87	310105	0.55			8.29
88	310202	0.73			9.85
89	310106	0.55			8.35
90	010203	0.18	0.18	2.0	7.04
91	010204	0.55			10.16
92	010205	0.73			11.78
93	010206	0.37			8.82
94	260201	0.18	0.18	2.5	9.39
95	260202	0.37			11.4
96	260203	0.55			12.40
97	260204	0.73			13.56

Free Air-lift

98	290301	0.64	NO	1.5	10.70
99	290302	0.82			11.80
100	290303	1.00			12.70
101	290304	1.19			13.30

103	020402	0.82	NO	2.0	12.17
104	020403	1.00			12.87
105	020404	1.19			14.00
106	040401	0.64	NO	2.5	14.50
107	040402	0.82			13.20
108	040404	1.19			15.60

#### MECHANICALLY AGITATED TANKS

SI.NO.	RUN CODE	% WT. RESIN	CONC. OF SOLUTION	RPM	$K_{SL} \text{ m/s} \times 10^5$
1	051001	0.5	0.002	1200	4.59
2	051002	0.4			4.83
3	051003	0.3			4.32
4	051004	1.0			3.78
5	051005	0.2			5.81
6	051006	0.1			6.6
7	091004	0.2	0.005		4.81
8	091005	0.5			3.95
9	091006	1.0			3.81
10	121002	0.4			4.30
11	121003	0.1			5.60
12	151001	0.3			4.67
13	131001	1.0	0.004		3.32
14	131002	0.5			3.53
15	131003	0.4			3.73
16	131004	0.3			4.09
17	131005	0.2			4.68
18	131006	0.1			4.94
19	141001	0.5	0.003		4.20
20	141002	1.0			3.20
21	141003	0.2			4.65
22	191001	1.0	0.005	1500	4.38
23	191002	0.5			5.49
25	191003	0.4			5.66
26	191004	0.3			5.90
27	191005	0.3			6.26
28	191006	0.2			6.8
29	221001	1.0	0.004		4.12
30	221002	0.5			5.14
31	221003	0.4			4.81
32	221004	0.3			5.55

33	221005	0.2	5.53	
34	221006	0.1	5.89	
35	311002	1.0	0.002	3.51
36	251001	0.5	4.74	
37	311001	0.4	5.34	
38	251002	0.3	4.71	
39	311003	0.2	6.00	
40	251003	0.1	8.01	
41	031101	0.5	5.30	
42	031102	1.0	3.30	
43	031103	0.2	5.53	

Sl.No.	CODE	TEMPERATURE	K <sub>SL</sub>	REMARKS
44	141206	10	3.38	1200RPM, 0.002N
45	141205	20	4.33	and 0.2% RESIN
46	141201	29	5.48	
47	141202	39	5.97	
48	141203	46	5.64	
49	141204	53	6.58	
Sl.No.	CODE	RPM	K <sub>SL</sub>	
50	301201	600	3.63	0.002N and 0.2%
51	261201	900	4.65	WITHOUT BAFFLES
52	261202	1200	5.49	
53	261203	1500	5.76	
54	261204	1650	5.99	
55	271201	1200	5.67	0.002N AND 0.2%
56	271202	1500	6.09	WITH BAFFLES
57	271203	900	5.13	
58	281202	1650	6.23	
59	301202	600	2.49	
60	301203	600	3.115	1200RPM, 0.005N
61	301204	900	4.50	and 0.5% RESIN
62	301205	1650	5.00	

## REFERENCES

1. P.Harriot, "Mass transfer to particles suspended in agitated tanks:Part 1", *AICHE Journal*, V8, 1962, p.93.
2. J.J.Barker & R.E.Treybal, "Mass transfer coefficients for solids suspended in agitated liquids", *AICHE Journal*, V6, 1960, p.289.
3. Y.Sano, N.Yamaguchi & T.Adachi, "Mass transfer coefficients for suspended particles in agitated vessels & bubble columns", *J. of Chem. Engg. Japan*, V7, 1974, p.255.
4. S.Boon-long, C.Laguerie & J.P.Coudrec, "Mass transfer from suspended solids to a liquid in agitated vessels", *Chem. Engg.Scie.*, V33, 1978, p.813.
5. N.Yagi, T.Motouchi & H.Akita, "Mass transfer from fine particles in stirred vessels, effect of specific surface area of particles", *Ind. Engg. Chem. Process Des. Dev.*, V23, 1984, p.145.
6. S.Asai, Y.Konishi & Y.Sasaki, "Mass transfer between fine particles and liquids in agitated vessels", *J. of Chem. Engg. Japan*, V21, 1988, p.107.
7. M.Levins and J.N.Glastonbury, *Trans. Inst. Chem. Engrs.*, V50, 1972, p.132.
8. S.Sanger and W.D.Deckwer, "Liquid -Solid mass transfer in Aerated suspensions", *The Chem. Engg. Journal*, V22, 1981, p.179.
9. S.V.Jadhav & V.G.Pangarkar, "Particle-liquid mass transfer in three phase sparged reactor", *The can. J. of Chem. Engg.*, V66, 1988, p.572.
10. S.V.Jadhav & V.G.Pangarkar, "Particle-liquid mass transfer in

characteristics of mixing impellers: part 1", *Chem. Engg. Progress*, V46, 1950, P.395.

21. D.L.J.Petrovic et al; "Mixing time in gas-liquid-solid draft tube air lift reactors", *Chem. Engg. Scie.*, V45, 1990, p.2967.
22. Y.Chisti & M.Moo young, "Improve the performance of air lift reactors", *Chem. Engg. Progress*, V38, 1993,
23. M.Y.Chisti, B.Halard & M.Moo young, "Liquid circulation in air lift reactors", *Chem. Engg. Scie.*, V43, 1988, p.451.
24. P.Weiland, "Influence of draft tube on operation behavior of air lift loop reactors", *Ger. Chem. Engg.*, V7, 1984, p.374.
25. G.G.Krishna Murthy, S.P.Mehrotra & A.ghosh, "Experimental investigation of mixing phenomena in gas stirred liquid bath, *Met. Trans.B*, V19B, 1988, p.839.
26. S.P.Mehrotra & A.K.Saxena, "Effects of processes variables on the residence time distribution of a solid in a continuously operated flotation cell", *International J. of Min. Proce.*, V10, 1983, p.255.
27. G.G.Roy et al., "Experimental studies on gas-liquid mass transfer in Pachuca tanks", Unpublished research, IIT Kanpur.